An intronic GAA repeat expansion in *FGF14* causes the autosomal-dominant adult-onset ataxia SCA50/ATX-FGF14

Graphical abstract

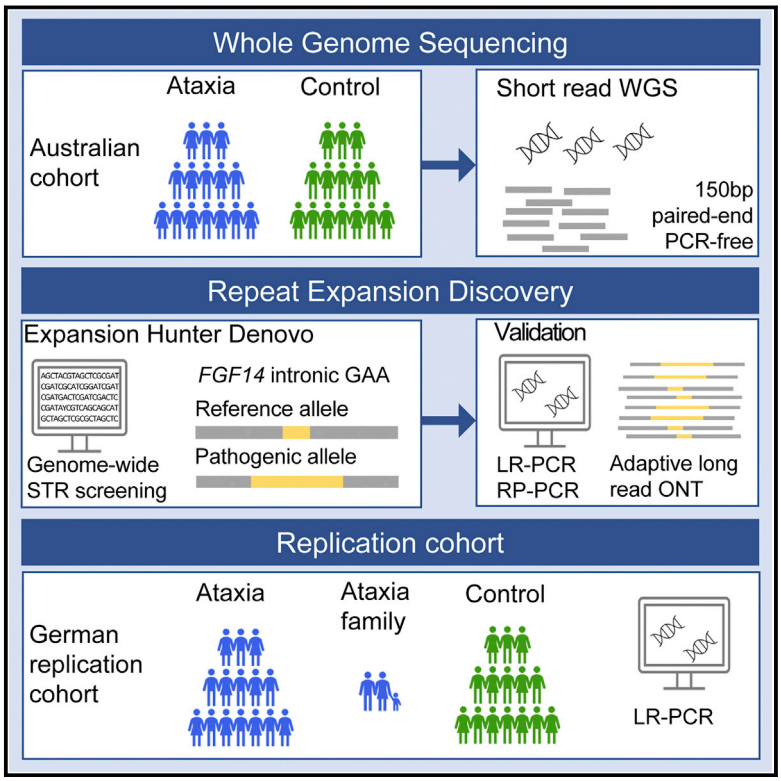

Authors

Haloom Rafehi, Justin Read, David J. Szmulewicz, ..., Martin B. Delatycki, Melanie Bahlo, Paul J. Lockhart

Correspondence

bahlo@wehi.edu.au (M.B.), paul.lockhart@mcri.edu.au (P.J.L.)

Pathogenic repeat expansions (RE) cause an array of neurogenetic disorders including cerebellar ataxia. While traditionally difficult to identify, new genomic tools and bioinformatic analyses are enabling rapid RE discovery and diagnosis. Here we characterize SCA50, an adult-onset ataxia caused by a pathogenic GAA repeat expansion within intron one of *FGF14*.

Rafehi et al., 2023, The American Journal of Human Genetics *110*, 105–119
January 5, 2023 Crown Copyright © 2022
https://doi.org/10.1016/j.ajhg.2022.11.015

An intronic GAA repeat expansion in *FGF14* causes the autosomal-dominant adult-onset ataxia SCA50/ATX-FGF14

Haloom Rafehi,[1,2,30] Justin Read,[3,4,30] David J. Szmulewicz,[5,6,30] Kayli C. Davies,[3,4] Penny Snell,[3] Liam G. Fearnley,[1,2,3] Liam Scott,[1] Mirja Thomsen,[7] Greta Gillies,[3] Kate Pope,[3] Mark F. Bennett,[1,2,8] Jacob E. Munro,[1,2] Kathie J. Ngo,[9] Luke Chen,[10] Mathew J. Wallis,[11,12,13] Ernest G. Butler,[14] Kishore R. Kumar,[15,16,17] Kathy HC. Wu,[18,19,20,21] Susan E. Tomlinson,[21,22] Stephen Tisch,[18,22] Abhishek Malhotra,[23] Matthew Lee-Archer,[24] Egor Dolzhenko,[25] Michael A. Eberle,[25] Leslie J. Roberts,[26] Brent L. Fogel,[9,28] Norbert Brüggemann,[7,27] Katja Lohmann,[7] Martin B. Delatycki,[3,4,29] Melanie Bahlo,[1,2,31,*] and Paul J. Lockhart[3,4,31,*]

Summary

Adult-onset cerebellar ataxias are a group of neurodegenerative conditions that challenge both genetic discovery and molecular diagnosis. In this study, we identified an intronic (GAA) repeat expansion in fibroblast growth factor 14 (*FGF14*). Genetic analysis of 95 Australian individuals with adult-onset ataxia identified four (4.2%) with $(GAA)_{>300}$ and a further nine individuals with $(GAA)_{>250}$. PCR and long-read sequence analysis revealed these were pure (GAA) repeats. In comparison, no control subjects had $(GAA)_{>300}$ and only 2/311 control individuals (0.6%) had a pure $(GAA)_{>250}$. In a German validation cohort, 9/104 (8.7%) of affected individuals had $(GAA)_{>335}$ and a further six had $(GAA)_{>250}$, whereas 10/190 (5.3%) control subjects had $(GAA)_{>250}$ but none were $(GAA)_{>335}$. The combined data suggest $(GAA)_{>335}$ are disease causing and fully penetrant ($p = 6.0 \times 10^{-8}$, OR = 72 [95% CI = 4.3–1,227]), while $(GAA)_{>250}$ is likely pathogenic with reduced penetrance. Affected individuals had an adult-onset, slowly progressive cerebellar ataxia with variable features including vestibular impairment, hyper-reflexia, and autonomic dysfunction. A negative correlation between age at onset and repeat length was observed ($R^2 = 0.44$, $p = 0.00045$, slope = −0.12) and identification of a shared haplotype in a minority of individuals suggests that the expansion can be inherited or generated *de novo* during meiotic division. This study demonstrates the power of genome sequencing and advanced bioinformatic tools to identify novel repeat expansions via model-free, genome-wide analysis and identifies SCA50/ATX-FGF14 as a frequent cause of adult-onset ataxia.

Introduction

Spinocerebellar ataxias (SCAs) are a heterogeneous group of progressive neurological disorders that are estimated to affect 1:33,000 individuals.[1] SCAs are caused by pathogenic expansions of short tandem repeats (STRs, also called microsatellites), in addition to deleterious point mutations. STRs are repeated nucleotide motifs of 2–6 base pairs (bp) that are known contributors to genetic polymorphism. There are ~239,000 STRs documented in the UCSC Genome Browser[2] and although current catalogs are incomplete,[3] STR loci are unstable and can rapidly mutate to alternative motifs or alter in length. Approximately 50 STRs have been shown to be pathogenic if they expand beyond locus-specific thresholds and result in repeat expansion (RE) disorders.[4] These include more common causes of ataxia, such as autosomal-dominant SCA 1, 2, 3, 6, and 7 and autosomal-recessive Friedreich

[1]Population Health and Immunity Division, The Walter and Eliza Hall Institute of Medical Research, Parkville, VIC 3052, Australia; [2]Department of Medical Biology, University of Melbourne, Parkville, VIC, Australia; [3]Bruce Lefroy Centre, Murdoch Children's Research Institute, Parkville, VIC 3052, Australia; [4]Department of Paediatrics, University of Melbourne, Royal Children's Hospital, Parkville, VIC, Australia; [5]Cerebellar Ataxia Clinic, Eye and Ear Hospital, Melbourne, VIC, Australia; [6]The Florey Institute of Neuroscience and Mental Health, University of Melbourne, Melbourne, VIC, Australia; [7]Institute of Neurogenetics, University of Lübeck, Lübeck, Germany; [8]Epilepsy Research Centre, Department of Medicine, University of Melbourne, Austin Health, Heidelberg, VIC, Australia; [9]Department of Neurology, David Geffen School of Medicine, University of California, Los Angeles (UCLA), Los Angeles, CA, USA; [10]Alfred Hospital, Department of Neurology, Melbourne, VIC, Australia; [11]Clinical Genetics Service, Austin Health, Melbourne, VIC, Australia; [12]Department of Medicine, University of Melbourne, Austin Health, Melbourne, VIC, Australia; [13]School of Medicine and Menzies Institute for Medical Research, University of Tasmania, Hobart, TAS, Australia; [14]Peninsula Health, Melbourne, VIC, Australia; [15]Faculty of Medicine and Health, The University of Sydney, Sydney, NSW, Australia; [16]Molecular Medicine Laboratory and Department of Neurology, Concord Repatriation General Hospital, Concord, NSW, Australia; [17]Garvan Institute of Medical Research, Sydney, NSW, Australia; [18]School of Medicine, University of New South Wales, Sydney, NSW, Australia; [19]Clinical Genomics, St Vincent's Hospital, Darlinghurst, NSW, Australia; [20]Discipline of Genomic Medicine, Faculty of Medicine and Health, University of Sydney, Sydney, NSW, Australia; [21]School of Medicine, University of Notre Dame, Sydney, NSW, Australia; [22]Department of Neurology, St Vincent's Hospital, Darlinghurst, NSW, Australia; [23]Department of Neuroscience, University Hospital Geelong, Geelong, VIC, Australia; [24]Launceston General Hospital, Tasmanian Health Service, Launceston, TAS, Australia; [25]Illumina Inc, San Diego, CA, USA; [26]Department of Neurology and Neurological Research, St. Vincent's Hospital, Melbourne, VIC, Australia; [27]Department of Neurology, University Medical Center Schleswig-Holstein, Campus Lübeck, Germany; [28]Departments of Human Genetics, David Geffen School of Medicine, University of California, Los Angeles (UCLA), Los Angeles, CA, USA; [29]Victorian Clinical Genetics Services, Melbourne, VIC, Australia
[30]These authors contributed equally
[31]These authors contributed equally
*Correspondence: bahlo@wehi.edu.au (M.B.), paul.lockhart@mcri.edu.au (P.J.L.)
https://doi.org/10.1016/j.ajhg.2022.11.015.

ataxia, as well as rarer forms such as SCA36 and 37. Many people presenting with ataxia receive a clinical diagnosis of idiopathic late-onset cerebellar ataxia (ILOCA)[5] or sporadic adult-onset ataxia (SAOA).[6] Ataxia may present with other clinical features, including neuropathy, vestibular dysfunction, parkinsonism, cognitive impairment, and psychiatric features, which may provide clues to an underlying genetic diagnosis. However, despite routine clinical testing for the more common causes of ataxia, only ~10%–30% of individuals with a clinical diagnosis of ataxia receive a genetic diagnosis.[7] This is thought to be in part due to as yet unidentified genetic causes, including REs, likely located in noncoding regions of the genome.[4]

The identification of pathogenic REs has historically been difficult. However, discovery and detection of complex genetic variants, such as REs, in genome-sequencing data have improved due to the advances in bioinformatic tools available to identify both known and novel (i.e., not present in the reference genome) RE.[8,9] Using these tools, we recently identified the RE that causes cerebellar ataxia with neuropathy and bilateral vestibular areflexia syndrome (CANVAS [MIM: 614575]), a common cause of adult-onset cerebellar ataxia.[10] This RE, a novel $(AAGGG)_n$ RE in *RFC1* (MIM: 102579), had previously evaded discovery despite presenting a well-defined recessive disease phenotype and a strong linkage region.

In this study we tested the hypothesis that advanced bioinformatic tools and second- and third-generation sequencing technologies provide an opportunity to perform model-free discovery of novel pathogenic REs in cohorts of unrelated individuals with overlapping but heterogeneous disorders. We identified a novel $(GAA)_n$ RE within intron 1 of *FGF14* (MIM: 601515) that appears to represent the most common genetic cause of adult-onset ataxia described to date.

Material and methods

Cohort recruitment and clinical phenotyping

The Royal Children's Hospital Human Research Ethics Committee (HREC 28097) and the Walter and Eliza Hall Institute of Medical Research (HREC 18/06) approved the study and all the procedures undertaken were in accordance with the ethical standards of the responsible committees. Individuals with suspected genetic cerebellar ataxia, based on clinical presentation, were recruited from multiple clinicians in Australia. Exclusion criteria were clinical features consistent with an acquired etiology, including onset of ataxia in association with acute injury or illness such as stroke, encephalitis, or sepsis. Informed consent was obtained from all 95 participants and details were collected from clinical assessments and review of medical records. Ancestry information was not collected. All participants were examined clinically by a consultant neurologist, with eight assessed by sub-specialist neuro-otologists. Cerebellar functional assessment included evaluation for gait ataxia, cerebellar dysarthria, and four-limb appendicular ataxia. Oculomotor assessment included documentation (in most) of any abnormal nystagmus, visual pursuit, and saccades to target. Brain MRI scans were assessed visually for regional cerebellar atrophy. Eight individuals underwent nerve conduction studies, but one of these had only lower limb studies. The other seven had motor studies of the median, ulnar, peroneal, and tibial nerves, including F-waves. Six of these seven participants also had upper limb sensory studies including antidromic and orthodromic median, ulnar, and radial digital studies while one person had limited upper limb sensory studies. All eight participants had antidromic sural and superficial peroneal sensory studies. Small nerve fiber studies were performed in six of the eight, with five having QSART testing and six having cutaneous silent period (CSP) studies. The QSART tests a population of C-fibers and the CSP studies test somatic Aδ fibers. Tilt table testing was undertaken in order to assess autonomic nervous system (ANS) function in four of the eight individuals.

The control cohort was composed of 215 unrelated adult individuals recruited from multiple sites in Australia, all healthy at the time of blood sampling (22–66 years of age). Informed consent was obtained, and all procedures were in accordance with the ethical standards of the Royal Children's Hospital Human Research Ethics Committee, Australia. Ancestry information was not collected but is likely similar to the proband cohort and overall reflect the diversity of backgrounds present in the Australian population. In addition, a panel of 96 lymphoblast-derived gDNA samples from UK control individuals, all healthy at the time of DNA sampling (24–65 years of age), were analyzed (HRC-1 control panel, Sigma Aldrich, #06041301, described by the manufacturer as of "Caucasian" ancestry).

A validation cohort of 104 unrelated individuals with ataxia of an unidentified cause and 190 control individuals from Lübeck, Germany, were included. The ethics committee of the University of Lübeck approved clinical assessments and genetic testing of this cohort (AZ16-039), informed consent was obtained and the procedures followed were in accordance with the ethical standards of this committee. The participants were recruited from the ataxia and vertigo outpatient clinic at the Department of Neurology, University Medical Center Schleswig-Holstein, Campus Lübeck. Vestibulo-oculography, calorimetry, NCS, and MRI were performed in a clinical setup. Some of the clinical MRI scans were not available for a personal review. In this case, information was derived from written reports.

Next generation sequence analysis

Genomic DNA was isolated from peripheral blood and genome sequencing was performed with the TruSeq PCR-free DNA HT Library Preparation Kit and sequenced on the Illumina NovaSeq 6000 platform. Genome-sequence (GS) data generated in-house from 210 unrelated control individuals from the Australian cohort (five samples failed to generate high-quality data) with no clinical evidence of ataxia was used for genetic studies. Targeted long-read sequencing of *FGF14* was performed using adaptive sampling on an Oxford Nanopore Technologies MinION Mk1B sequencer. Blood-derived genomic DNA was used to construct sequencing libraries using the manufacturer's specifications including the NEBNext Companion Module (New England BioLabs) and SQK-LSK110 Ligation Sequencing Kit (Oxford Nanopore Technologies). FLO-MIN106D flow cells (Oxford Nanopore Technologies) were loaded with library and run for 24 h before being washed using the Flow Cell Wash Kit (EXP-WSH004, Oxford Nanopore Technologies) and reloaded with additional library for a further 24 h. Sequencing with adaptive sampling was performed by Readfish (v.0.0.2),[11] with the entire gene and a 100 kb flanking region

selected for adaptive sequencing enrichment (hg38 chr13: 101,610,804–102,502,457).

Alignment and variant calling and STR analysis

For short-read data, alignment was performed based on the GATK best practice pipeline.[12,13] Fastq files were aligned to the hg38 reference genome using BWA-mem, then duplicate marking, local realignment, and recalibration was performed with GATK. The RE detection tools exSTRa[14] (v.1.1.0) and ExpansionHunter[15] (v.5.0.0) were used to screen for known pathogenic REs using default parameters. A database of pre-defined pathogenic REs was used (exSTRa in web resources, file version committed on June 26, 2020). These tools utilize paired-end reads to detect expanded STRs: exSTRa uses an empirical cumulative distribution function (ECDF) to determine outliers, while ExpansionHunter estimates the number of repeats in the STR on each allele. Novel RE discovery was performed for known ataxia-associated genes (candidate gene list curation described below) using ExpansionHunter Denovo[9] (EHDN, v.0.9.0) using the outlier method (max-irr-mapq = 60), comparing 47 individuals with ataxia to 210 control subjects with high-quality GS. RE were excluded from further analysis if they were intergenic or only called outliers in only a single ataxia case. EHDN was also used, with default parameters, to profile genome sequence data from the 1000 Genomes Project.[16] Analysis was performed on the publicly available 1000 Genomes 30x on GRCh38 data collection.[17] Sample metadata, including pedigree information and ethnicity, was obtained from the metadata provided by the 1000 Genomes Project.[16]

Related individuals were removed from the analysis, leaving 2,483 individuals from diverse ethnic backgrounds. We used nf-cavalier, an in-house Nextflow Pipeline,[18] for screening of SNP and indel variants in the Australian cohort (cavalier in web resources). The pipeline utilizes GATK variant calls,[19] bcftools,[20] IGV,[21] and ensembl VEP[22] annotations. Variants were filtered according to the following criteria: minimum VEP impact "MODERATE;" maximum cohort allele frequency 0.3; and present on a curated ataxia gene list. Candidate genes were selected from published ataxia gene panels curated by PanelApp Australia and PanelApp UK. Additional genes were obtained from OMIM with a phenotype referencing ataxia. Dominant, recessive, and compound heterozygous inheritance patterns were further filtered using VEP provided gnomAD allele frequencies (AF) as follows: AF dominant ≤ 0.0001, AF recessive ≤ 0.01, AF compound heterozygous ≤ 0.01. IGV screenshots of putative variant calls were then reviewed manually. For the long-read data, base-calling was performed using the Guppy basecaller with a super-accuracy base-calling model (v.6.2.3, Oxford Nanopore Technologies). STR analysis was performed using tandem genotypes[23] (v.1.90) after alignment with LAST (v1409). A common ancestral haplotype was determined for three Australian participants with $(GAA)_{>250}$ by comparing variant sharing around the *FGF14* STR for variations with a gnomAD AF < 0.1 using short-read sequencing data.

Molecular genetic studies

We designed a long-range PCR (LR-PCR) assay to test the size of the *FGF14* STR utilizing Phusion Flash High-Fidelity PCR Master Mix (ThermoFisher Scientific, F548). The primers (Table S1) flank the STR and are predicted to amplify a 315 bp fragment based on hg38 reference sequence, which includes 50 GAA repeats. PCR was performed in a 20 μL reaction with 50 ng genomic DNA and 0.1 μM of forward and reverse primers. A standard 35 cycle PCR protocol was utilized (98°C denaturation for 1 s, 63°C anneal for 10 s, and 72°C extension for 2 min). Products were visualized using agarose gel electrophoresis and fragment analysis of FAM labeled PCR products was performed on capillary array (ABI3730xl DNA Analyzer, Applied Biosystems) and visualized using PeakScanner 2 (Applied Biosystems). The presence of an expanded *FGF14* RE was tested by repeat-primed PCR (RP-PCR) utilizing three primers; FGF14_RPP_ F1_FAM (0.1 μM), FGF14_RPP_AAG_RE_R1 (0.2 μM), and RPP_M13R (0.1 μM, Table S1), with the cycling conditions and analysis described above.

Genetic analysis of the validation cohort

The validation cohort consisted of 104 unrelated individuals with ataxia, 190 control subjects, and two healthy parents of one affected individual. All samples were collected at the University of Lübeck and were predominantly of German ethnicity. LR-PCR was applied to these 296 individuals with the primers listed in Table S1 using a standard PCR protocol with an extension time of 2 min. Products were separated on an automated sequencing machine (Genetic Analyzer 3500XL, Applied Biosystems) using a LIZ1200 size standard. LR-PCR products of samples that appeared to be homozygous (only one allele visible) or carriers of alleles of >900 bp (~250 repeats) were also separated on an 1% agarose gel to exclude or confirm the presence of expanded alleles. Specificity of the PCR products was confirmed by Sanger sequencing of the repeat-flanking region.

Statistical analyses

Linear regression was performed in R (v.4.0.5) using the base function [lm()] to determine the correlation between age at onset and RE expansion length. A linear equation was determined from the output of the lm function. Fisher exact test was used to test for enrichment of *FGF14* RE $>(GAA)_{250}$ in affected individuals versus control subjects.

Results

Participant recruitment

The workflow for this study is summarized in Figure 1. In the first step, 47 adults with ataxia were recruited and underwent short-read genome sequencing, in addition to subsequent LR-PCR and RP-PCR analysis. All were singletons without a verified family history of ataxia. Second, an additional Australian cohort of 48 individuals was recruited and analyzed by LR-PCR and RP-PCR only. All individuals (n = 95) were diagnosed with ataxia based on clinical examination by a neurologist and included 53 female/42 male individuals with adult-onset ataxia (mean age at onset 54 ± 14 years, range 24–72 years). Individuals were excluded if there was clinical suspicion of an acquired cause of ataxia, based on history of acute injury or illness, toxic exposure, or rapid onset. Screening for the pathogenic REs in the genes associated with SCA1, SCA2, SCA3, SCA6, and SCA7 was performed by diagnostic ataxia panel testing prior to research-based genetic testing.

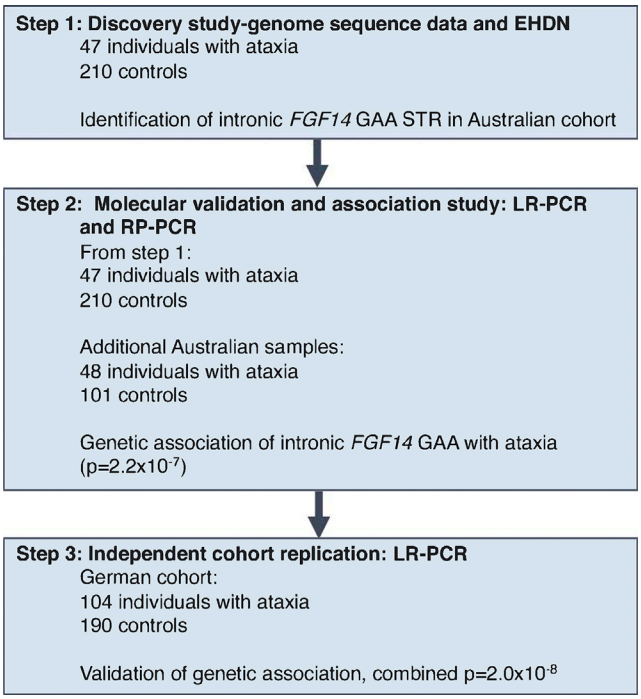

Figure 1. Overview of the study and investigations performed

Discovery of a novel repeat expansion in *FGF14*

Given the enrichment of REs as a genetic cause of ataxia, the sequence data of the 47 affected individuals (discovery cohort) was screened for novel REs using ExpansionHunter De novo (EHDN), compared to 210 unrelated control subjects. This analysis identified enrichment of an expanded GAA repeat in intron 1 of *FGF14* in participants versus control subjects, with an outlier *Z* score of 17.48 and was the second candidate on the list. The top candidate was the GAA in *FXN*, an STR already known to cause Friedreich's ataxia. Point mutations resulting in haploinsufficiency for *FGF14* are a known rare cause of autosomal-dominant spinocerebellar ataxia 27 (SCA27 [MIM: 193003]),[24] but REs in this gene have not been previously identified. The $(GAA)_n$ STR is located in the hg38 reference genome at chr13:102,161,577–102,161,726 and is reported to consist of 50 pure GAA motifs. Plotting anchored in-repeat reads (a-IRR) from EHDN shows that the STR is present in affected individuals and control subjects, with seven outliers from the affected individuals (a-IRR > 30, Figure 2A) compared to 210 control subjects (Figure 2B). Large a-IRRs are correlated with longer expansion.[9] EHDN detected the STR in 21 of 47 affected individuals (44.7%) and 67 of 210 control subjects (31.9%). The individuals in which zero value a-IRR was reported either do not have the *FGF14* STR, or it is < 150 bp (50 repeats) in length as this is the minimum size detectable by EHDN (see below). Visualization of the genome sequence reads in IGV confirmed the likely presence of an expanded $(GAA)_n$ STR in intron 1 of *FGF14* (Figure S1). To further characterize the locus prior to proceeding to molecular validation, genome sequence data was analyzed with exSTRa and ExpansionHunter (Figure S2). Results from exSTRa (Figure S2A) indicate that a $(GAA)_n$ STR exists at the locus in a range of sizes in the general population, with many control subjects displaying a high proportion of reads containing full 150 bp-reads of GAA repeats. As a result, outlier analysis using exSTRa is not feasible for this locus. In addition, genotyping with ExpansionHunter identifies $(GAA)_n$ REs in the 100 repeat range in both affected individuals and control subjects, although density plots indicate a shift in the distribution toward larger repeats in the affected individuals (Figure S2B).

Molecular validation of the *FGF14* GAA RE

To confirm expansion of the $(GAA)_n$ STR, we performed standard PCR and agarose gel electrophoresis of two affected individuals identified by EHDN and two control subjects predicted to not be expanded. This analysis demonstrated additional products >1,000 bp in the affected individuals, whereas the control subjects only showed products less than 300 bp (Figure 3A). The predicted PCR product size based on hg38 is 315 bp, which includes $(GAA)_{50}$. We then developed locus-specific LR-PCR and RP-PCR assays to investigate the size and motif composition of the *FGF14* STR by capillary array analysis. Consistent with the standard PCR assay, LR-PCR analysis identified a heterozygous expanded allele in both affected individuals, with estimated larger allele sizes of $(GAA)_{289}$ and $(GAA)_{349}$, respectively (Figure 3B). In comparison, estimated allele sizes of $(GAA)_{22}$ and $(GAA)_{12}$ were observed in the control subjects, matching the standard PCR results. Similarly, we observed an extended saw-toothed "ladder" in affected individuals when the RP-PCR products were analyzed by capillary array, which was absent in control subjects (Figure 3C). These results suggest that EHDN had correctly identified a novel heterozygous $(GAA)_n$ RE in intron 1 of *FGF14* and validated molecular tools were applied to perform genetic characterization in the larger cohort.

We then performed LR-PCR analysis of all 95 affected individuals and 311 control subjects, which included an additional 48 affected individuals with no genome-sequence data. In total, we identified 13 affected individuals with an allele greater than $(GAA)_{250}$, four of which were $(GAA)_{>335}$ (Figure 4A, Table S3). Analysis of the available genome data (eight individuals) with EHDN confirmed the presence of large *FGF14* $(GAA)_n$ expansions. In addition, we screened for pathogenic RE known to cause ataxia using ExpansionHunter and exSTRa, and for pathogenic sequence and copy number mutations in known ataxia-associated genes. No candidate pathogenic variants were identified in these eight individuals. LR-PCR demonstrated only five control subjects had an allele greater than $(GAA)_{250}$, with the maximum size being $(GAA)_{300}$. Comparison of allele size estimates by ExpansionHunter and LR-PCR revealed bioinformatic sizing of the RE using short-read GS data was significantly underestimated when the *FGF14* RE was greater than $\sim(GAA)_{100}$

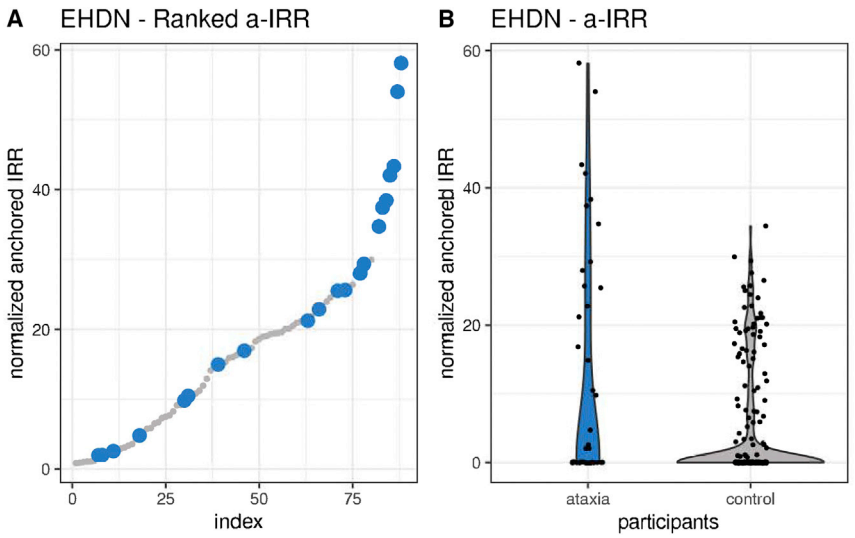

Figure 2. RE analysis with EHDN identifies a potentially pathogenic novel intronic GAA RE in *FGF14* enriched in the ataxia cohort

(A) Summary of ranked anchored-IRR findings for affected individuals (blue) and control subjects (gray) for the intronic GAA STR in *FGF14*.

(B) Violin plot showing the difference in distribution of the anchored-IRR for affected individuals (blue) and control subjects (gray) for all individuals with an *FGF14* repeat motif of at least $(GAA)_{50}$. Anchored-IRR for individuals with a repeat less than $(GAA)_{50}$ are not detected by EHDN; hence, not all individuals analyzed are represented in these plots.

(Figures 4B and 4C). Interestingly, LR-PCR and RP-PCR revealed a consistent symmetrical peak distribution for all 13 affected individuals with an allele greater than $(GAA)_{250}$ (Figures 3B and 3C), suggestive of a pure $(GAA)_n$ RE. This was confirmed by long-read sequencing (Figure S3), with expanded reads in all five samples analyzed with an RE > $(GAA)_{250}$ being pure GAA. In addition, this analysis also confirmed the RE sizes observed by LR-PCR, with estimates for the two methods differing by less than 5%. In comparison, three of five controls with estimated RE sizes of $(GAA)_{332}$, $(GAA)_{296}$, and $(GAA)_{282}$ displayed unusual LR-PCR peaks (Figure 4D) and RP-PCR traces (Figure 4E). Inspection of the short-read sequence data for these control subjects clearly demonstrated that the RE was not made up of pure GAA motifs, but instead appeared to consist of GAAGGA hexamer repeats (Figure S4). It is well established that interrupted and impure RE can modify disease penetrance and severity in other autosomal-dominant SCA[25–27] and our analysis raises the possibility that this may apply to disease mediated by GAA expansion in *FGF14*. Considering only pure expanded $(GAA)_n$ STRs, we identified 13 affected individuals (13.7%) with an allele greater than $(GAA)_{250}$, but only two control subjects (0.6%), with pure repeats of $(GAA)_{272}$ and $(GAA)_{300}$, respectively (Figure 4A). Collectively, these data suggest that heterozygous expansion of a pure GAA repeat within intron 1 of *FGF14*, beyond a threshold of ~250 motifs, represents a common cause of adult-onset ataxia (Fisher's exact test $p = 2.2 \times 10^{-7}$, OR = 24.3 [95% CI = 5.3–224.7]). Pure alleles $(GAA)_{>300}$ were exclusively found among affected individuals (n = 8) in the Australian cohort.

To test the frequency of the $(GAA)_n$ RE in additional populations, we screened a German cohort of 104 individuals with adult-onset ataxia using LR-PCR (Table S2). This analysis identified 15 affected individuals (14.4%) with an allele greater than $(GAA)_{250}$, compared to 10/190 (5.3%) observed in control subjects (Fisher's exact test p = 0.014, OR = 3.03 [95% CI = 1.3–7.02]). Given the differences in the frequency of $(GAA)_{>300}$ in Australian (0/311) and German (7/190) control subjects, we initially analyzed the combined dataset with stringent criteria, requiring the pathogenic cutoff to be greater than the largest observed control allele [$(GAA)_{332}$]. The results suggest that expanded alleles greater than $(GAA)_{332}$ are pathogenic and fully penetrant ($p = 6.0 \times 10^{-8}$, OR = 72 [95% CI = 4.3–1,227]). Similarly, analyzing the combined dataset using the lower size threshold established in the Australian cohort suggests that alleles in the range of $(GAA)_{250\text{-}334}$ are likely to be pathogenic (p = 0.0015, OR = 3.6 [95% CI = 1.6–7.9]), albeit with reduced penetrance.

Large repeats in other SCA are known to be unstable and demonstrate intergenerational variability. For one index participant, DNA samples were also available from clinically unaffected parents, allowing evaluation of germline repeat instability. We observed no change in the size of the paternal $(GAA)_{25}$ allele, whereas the maternal allele increased from $(GAA)_{282}$ to $(GAA)_{315}$ (Figure S5). This observation provides anecdotal evidence of meiotic instability of expanded alleles and incomplete penetrance of $(GAA)_{>250}$.

Profiling of *FGF14*-GAA in 1000 genomes project data

Next, we applied EHDN to data from the 1000 Genomes Projects to further characterize the composition of the *FGF14* STR locus in diverse populations. EHDN only analyzes reads that contain a pure motif and that are >150 bp, so any STRs that are shorter than the read length (i.e., <150 bp/50 triplet repeats) are not detected by EHDN. We found that the *FGF14* STR > $(GAA)_{50}$ is present in all five super populations represented in the 1000 Genomes project with frequencies of African (8%), admixed American (22.4%), East Asian (8.5%), South Asian (24.1%), and European (32.3%) (Figure S6A). Furthermore, European and South Asian populations have higher a-IRR on average, while African populations have the lowest counts of a-IRR (Figure S6B), indicating that longer forms of the

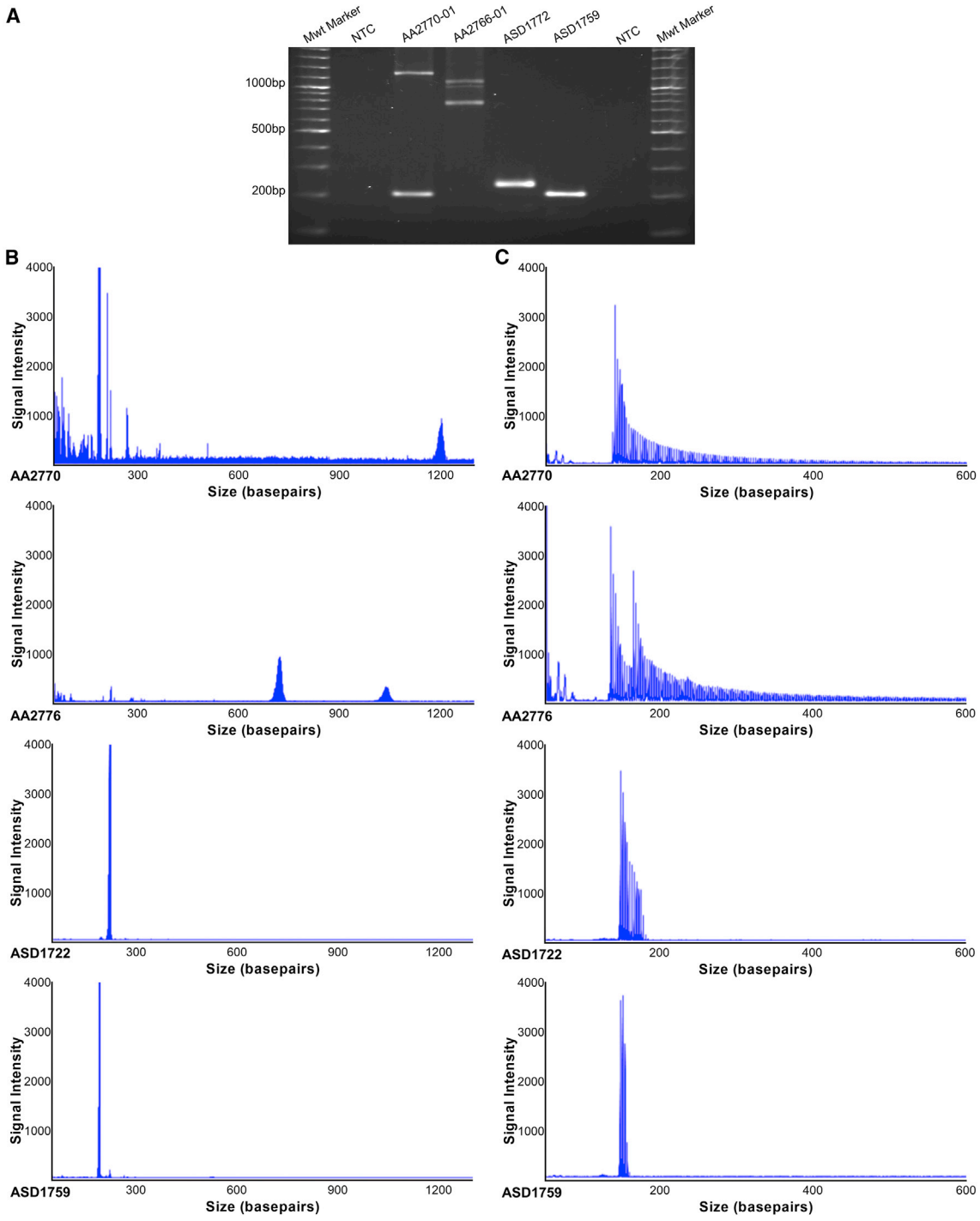

Figure 3. Molecular validation confirms a heterozygous (GAA) RE in *FGF14*

(A) Gel electrophoresis of PCR products spanning the *FGF14* (GAA) STR locus. Affected individuals (AA2770 and AA2766) produced large PCR products of between ~1,000 bp and ~1,200 bp compared to control subjects (ASD1722 and ASD1759 <~300 bp). No product was observed in the no-template negative control (NTC).

(B) Accurate quantification of (GAA) repeat size was determined by fragment analysis. Individuals with large GAA expansions generated low signal intensity peaks, with staggered peak formations in 3 bp intervals >~1,000 bp, indicating an allele with a high number of repeats. Electropherograms of non-expanded LR-PCR products displayed a single high intensity spike at <300 bp.

(C) RP-PCR for the (GAA) RE demonstrated an extended saw-toothed product with three base pair repeat unit size in affected individuals that was truncated or absent in control individuals.

STR are present across populations but in different frequencies. In addition, while $(GAA)_n$ is by far the most common, EHDN also identified population-specific alternative motifs that are variations of GAA, including GAAGGA and GAAGAAGAAGAAGCA, both of which are present in East Asian and admixed American populations (Figure S6C).

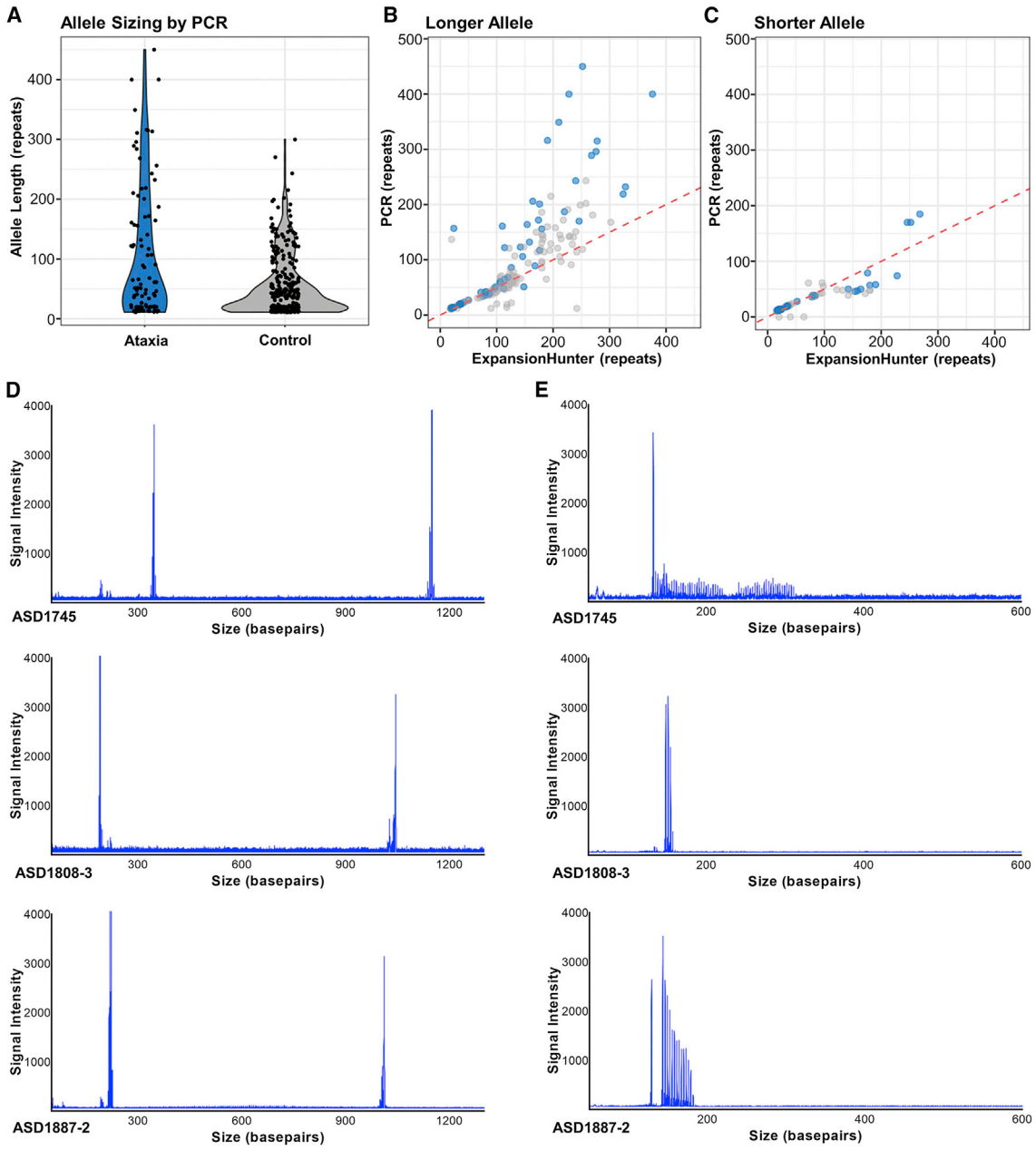

Figure 4. Characterization of *FGF14* (GAA) RE in study participants

(A) The allele size of the *FGF14* $(GAA)_n$ STR was determined in all available affected individuals (n = 95) and control subjects (n = 311) using fragment analysis of LR-PCR products. Allele size frequency is indicated on the violin plots, with greater frequency represented by a wider distribution. Thirteen affected individuals demonstrated pure $(GAA)_{>250}$, compared to only two control subjects.

(B and C) Comparison of *FGF14* (GAA) repeat length as determined by LR-PCR and ExpansionHunter for the longer (B) and shorter (C) allele demonstrated ExpansionHunter consistently under-estimates repeat size in comparison to molecular sizing (affected individuals [clear blue] and control subjects [clear gray]). The dotted red line indicates the y = x relationship representing equivalent sizing. Areas of darker blue indicate overlapping points.

(D) Electropherograms from three controls with $(GAA)_{>250}$ display an unusual pattern, with a single high-intensity peak observed corresponding to the large allele.

(E) RP-PCR analysis demonstrated inconsistent and stunted peak patterns, as opposed to the expected sawtooth "ladder." This pattern is consistent with an impure/alternate repeat motif.

Analysis of *FGF14* expression in primary fibroblast lines

Two predominant mRNA isoforms are produced by *FGF14*, which result from usage of different first exons. The primary site of expression of the longer isoform (1b) is the brain, with high levels observed in the cerebellum and cortex.[28] The $(GAA)_n$ RE is located within intron 1 of isoform 1b (Figure S7). Therefore, it is possible that the *FGF14* RE can interfere/reduce gene transcription, analogous to how expansion of the only other known (GAA) RE, located in intron 1 of *FXN*, reduces *FXN* expression and causes

Friedreich ataxia (FRDA [MIM: 229300]).[29] Reduced expression of the mutant *FGF14* allele could lead to haploinsufficiency, the disease mechanism underlying SCA27, caused by heterozygous mutations in *FGF14*.[24] To test this, we generated primary fibroblasts from three affected individuals with $(GAA)_{244}$, $(GAA)_{289}$, and $(GAA)_{348}$. Expression of both isoforms 1a and 1b is reported to be very low in fibroblast cell lines (GTEx) and indeed we were unable to reliably detect either isoform using TaqMan Gene Expression Assays and standard qRT-PCR or ddPCR, the latter being an extremely sensitive tool for absolute quantitation of gene expression.[30] Similarly, Western blot analysis failed to identify FGF14 in protein extracts from participant or control lines, reflecting the low gene expression (data not shown).

Clinical findings

A pure *FGF14* RE $>(GAA)_{250}$ was identified in 13 Australian individuals with cerebellar ataxia (CA). The sex distribution was 5 female to 8 male and mean age at symptom onset was 61 years (range 46–77 years). Participants were evaluated at a mean age of 69 years (range 54–81) after a mean period of 8.5 years (range 1–16) since symptom onset. All displayed a range of clinical ataxic phenomena, with MRI scanning revealing cerebellar atrophy in five of the 13 (Table 1). Six of 10 assessed had evidence of vestibular hypofunction on video head impulse test (vHIT),[31] five were bilaterally hypoactive, and one was unilaterally hypoactive. An abnormal video visually enhanced vestibulo-ocular reflex (VVOR) was seen in those with bilateral vestibular hypofunction.[32] Where formally assessed with a pure tone audiogram, four of 10 had hearing loss consistent with presbycusis, four of 10 with noise-induced hearing loss (HL), one had unilateral post-traumatic HL and one had early-onset HL (the details of which were unavailable). Additional extracerebellar features are described in Table 1.

Neurophysiology

Both motor and sensory studies were normal in the six affected individuals in whom a detailed nerve conduction study was performed (Table 1), apart from two who had focal median motor and sensory slowing across the wrists, indicating asymptomatic median neuropathies at the wrists (i.e., asymptomatic carpal tunnel syndrome). The findings were normal in the individual who had only lower limb studies. The findings in the one individual who had lower limb studies and limited upper limb studies were normal apart from an asymptomatic median neuropathy at the wrist. Small nerve fiber studies were normal in the six affected individuals in whom they were performed and provided no evidence of a somatic small fiber neuropathy. All four individuals who underwent tilt table testing had borderline to mild asymptomatic orthostatic falls of the systolic blood pressure of 18–37 mmHg. One of these individuals who also had a reduced heart rate response to deep breathing and standing was taking anti-hypertensive medication at the time of testing and, given this potential confound, we can only conclude that three displayed evidence of orthostatic hypotension. In addition, one participant had a reduced heart rate response to deep breathing and standing. Overall, the neurophysiology investigations failed to show consistent evidence of somatic large or small fiber neuropathy or neuronopathy. The tilt table and autonomic testing suggests likely involvement of the autonomic nervous system.

Age at onset analysis

RE length is often inversely correlated with disease age at onset. We applied a linear regression model to determine the relationship between *FGF14* RE length and ataxia onset age for the individual cohorts and also for the pooled data (Figure S8A). This analysis identified an inverse correlation ($R^2 = 0.44$, $p = 0.00045$, slope $= -0.12$). The regression suggests that for every $(GAA)_{10}$ increase above 250 repeats, the age of onset is reduced by ~1.16 years. Similar results were observed when the Australian ($R^2 = 0.36$, $p = 0.038$, slope $= -0.10$) and German ($R^2 = 0.55$, $p = 0.0058$, slope $= -0.14$) cohorts were analyzed independently (Figures S8B and S8C).

Discussion

Cerebellar ataxia (CA) may be defined as a disturbance of the normal co-ordination of movements and comes about when there is an impairment of cerebellar function. CA have multiple etiologies and many are associated with progressive and debilitating illness. Pathogenic repeat expansions collectively represent the most common genetic cause of CA and while they have traditionally proven difficult to both discover and assess diagnostically using standard molecular tools and practices, recent advances in genomic technologies have begun to address these limitations.[33,34] Here we demonstrate the power of new bioinformatic tools and second and third generation sequencing platforms by identifying and characterizing a novel pathogenic $(GAA)_n$ RE within intron 1 of *FGF14* in a significant proportion of unresolved individuals with adult-onset ataxia. We replicate the initial finding made in an Australian cohort in an independent German cohort. Interestingly, seven $(GAA)_{301\text{-}332}$ alleles were observed in German control subjects, compared to none in the Australian samples. This may reflect a difference in population structure or the fact that some of these may represent non-pure alleles, which were identified and removed from the Australian dataset. Irrespective, our data strongly support a fully penetrant threshold of $(GAA)_{>335}$ for this RE and also supports $(GAA)_{>250}$ as likely pathogenic, albeit with reduced penetrance. However, defining the pathogenic range will require additional, larger studies in aged control subjects since the disease onset can occur very late in life; onset ages of 70 and 77 years were observed in our cohorts. Given that de-identified DNA samples for

Table 1. Clinical features of individuals with *FGF14* GAA expansion

		Demographics				Cerebellar clinical features						Vestibular function	Neurophysiology		MRI		
ID	$(GAA)_n$ size	Sex	Age at onset (y)	Age at assessment (y)	Disease duration (y)	Upper limb ataxia	Lower limb ataxia	Gait ataxia	Oculomotor abnormalities	Truncal ataxia	Cerebellar dysarthria	Hypofunction on vHIT	Sensory +/or motor impairment on NCS	Autonomic nervous system dysfunction	Cerebellar, brain stem, or other atrophy	Extracerebellar features	Core phenotype
AA2807	450	M	47	57	10	+	+	+	+	+	+	ND	–	ND	–	–	CA[a]
AA2903	>400	F	58	68	10	+	+	+	+	–	+	unilateral	–	+	–	hyper-reflexia	CAUV, ANS and hyper-reflexia
AA2831	>400	M	ND	66	ND	–	ND	+	ND	ND	ND	ND	ND	ND	anterior cerebellar atrophy	spasticity	CA[b]
AA2770	348	F	55	71	16	+	+	+	+	–	+	–	–	ND	superior and posterior vermal, mild hemispheric atrophy	chronic cough	CA and cough
AA0441	317	M	65	71	6	+	+	+	+	–	+	–	–	ND	–	–	CA
AA2895	312	M	46	54	8	–	+	+	+	–	ND	ND	ND	ND	generalized cerebellar atrophy, principally vermis	lower limb hyper-reflexia, spasticity	CA[a] and spasticity
AA2775	310	M	58	68	10	+	+	+	+	–	+	bilateral	–	+	anterior and posterior vermal, mild hemispheric atrophy	lower limb hyper-reflexia	CABV, ANS and hyper-reflexia
AA2809	309	M	70	74	4	+	–	+	+	–	–	bilateral	–	+[c]	–	lower limb hyper-reflexia, parkinsonism	CABV, hyper-reflexia and parkinsonism
AA2845	298	F	69	70	1	–	–	+	+	–	–	–	–	ND	–	–	CA
AA2766	289	M	62	73	11	+	+	+	+	–	+	bilateral	–	+	superior and posterior vermal, mild hemispheric atrophy	chronic cough	CABV, ANS and cough
AA2908	281	F	59	74	15	+	+	+	+	+	+	bilateral	ND	ND	–	clinical ANS dysfunction	CABV and clinical ANS
AA2933	280	F	77	81	6	–	–	+	+	–	–	–	ND	ND	–	–	CA
AA2926	270	M	67	73	6	+	+	+	+	–	–	bilateral	ND	ND	–	–	CABV

(*Continued on next page*)

Table 1. ***Continued***

		Demographics				Cerebellar clinical features						Vestibular function	Neurophysiology		MRI		
ID	**$(GAA)_n$ size**	**Sex**	**Age at onset (y)**	**Age at assessment (y)**	**Disease duration (y)**	**Upper limb ataxia**	**Lower limb ataxia**	**Gait ataxia**	**Oculomotor abnormalities**	**Truncal ataxia**	**Cerebellar dysarthria**	**Hypofunction on vHIT**	**Sensory +/or motor impairment on NCS**	**Autonomic nervous system dysfunction**	**Cerebellar, brain stem, or other atrophy**	**Extracerebellar features**	**Core phenotype**
L-18362	~460	M	ND	71	ND	+	+	+	+	+	+	bilateral	–	ND	cerebellar atrophy, primarily, superior vermis	spasticity	CABV and spasticity
L-17665	~430	F	46	51	5	–	–	–	+	–	–	bilateral	–	ND	–	–	CABV
L-17672	~430	M	54	56	2	–	+	+	+	–	–	–	–	ND	–	–	CA
L-18384	~430	M	60	64	4	–	–	+	+	–	–	bilateral	–	ND	ND	–	CABV
L-20363	~400	M	60	85	25	+	+	+	+	ND	–	unilateral	–	ND	ND	–	CAUV
L-15166	~350	M	<41	46	>5	+	+	+	+	ND	+	ND	ND	ND	frontal atrophy	spasticity	CA[a], spasticity
L-15764	~350	M	63	70	7	+	+	+	+	+	+	bilateral	–	ND	moderate global atrophy, predominantly cerebellar	–	CABV
L-14630	~340	M	54	75	21	–	–	+	+	–	–	ND	ND	ND	–	clinical ANS dysfunction	CA[a] and clinical ANS
L-10410	~320	F	ND	ND	ND	ND	ND	+	ND	ND	ND	ND	ND	ND	ND	ND	CA
L-15891	~310	M	70	75	5	+	+	+	–	ND	–	bilateral	ND	ND	–	clinical ANS dysfunction	CABV and clinical ANS
L-15754	~290	F	74	84	10	+	+	+	+	ND	–	bilateral	ND	ND	–	clinical ANS dysfunction	CABV and clinical ANS
L-14575	~290	M	60	81	21	+	ND	+	+	ND	+	bilateral	ND	ND	ND	sensory neuropathy	CABV, neuropathy
L-15713	~270	M	74	76	2	+	+	+	+	+	+	bilateral	–	ND	global brain and cerebellar atrophy	clinical ANS dysfunction	CABV and clinical ANS
L-15739	~270	F	75	77	2	–	–	+	+	ND	–	bilateral	–	ND	global brain atrophy	–	CABV
L-15629	~270	M	76	83	7	+	+	+	+	+	–	–	ND	ND	global brain and cerebellar atrophy	–	CA

vhit, video head impulse test; NCS, nerve conduction study; ANS, autonomic nervous system; M, male; F, female; +, present; −, absent; ND, no data available; CA, cerebellar ataxia; CABV, cerebellar ataxia and bilateral vestibulopathy; CAUV, cerebellar ataxia and unilateral vestibulopathy.

[a]vHIT not performed.

[b]cerebellar ataxia no other phenotypic information available.

[c]present on anti-hypertensive medication.

"healthy" control subjects, such as the HRC1 panel used in this study, are often acquired many years prior to potential disease onset, it is difficult to determine if an expanded allele is non-penetrant, below a "pathogenic" threshold, or simply that the individual is yet to manifest the condition. In addition, this study has highlighted the likely need to determine both the size and structure (repeat sequence) of expanded *FGF14* alleles as a part of molecular diagnosis. Achieving a genetic diagnosis confers a number of benefits including definitive diagnosis, improved prognostication, possible implications for reproductive choices, and identification of gene therapy targets. We anticipate increasing application of third generation (long-read) sequencing technologies in diagnostic facilities to meet the challenges of accurate genetic diagnosis for *FGF14* and indeed the majority of RE-mediated disorders. We demonstrate that *FGF14* can be efficiently targeted and screened with the adaptive sampling technique afforded by ONT sequencing.

While this study has a cross-sectional cohort design, our results suggest that *FGF14* RE-mediated disease can result from either *de novo* expansion or familial inheritance of an expanded pathogenic allele. Three individuals share a core haplotype spanning ~395 kbp, suggesting distant relatedness and inheritance of a founder RE. Indeed, the haplotype includes rs72665334, a single-nucleotide variant identified by GWASs as associated with down beat nystagmus (DBN).[35] Given that DBN is the most common form of abnormal central nervous system-mediated nystagmus[36] and is observed in a broad range of CAs, it is not surprising that it is a feature of *FGF14* RE-mediated disease. However, the haplotype result raises the intriguing possibility that DBN-associated rs72665334, present in the global population with an aggregate allele frequency of ~5% (dbSNP-ALFA), is actually the result of the variant being on a founder haplotype in linkage disequilibrium with a *FGF14* $(GAA)_n$ RE. Although this study does not include *FGF14*-linked multiplex families to determine intergenerational RE stability, our analysis of control cohorts and the 1000 Genomes Project (Figures 4 and S6) has demonstrated that the *FGF14* $(GAA)_n$ STR is highly polymorphic in the population. Moreover, we observed intergenerational expansion of a $(GAA)_{282}$ allele in an unaffected female to $(GAA)_{315}$ in her affected daughter (Figure S5).

Members of the FGF family possess broad mitogenic and cell survival activities and are involved in a variety of biological processes, including embryonic development, morphogenesis, tissue repair, tumor growth, and invasion. *FGF14*, and in particular isoform 1b, is widely expressed in the developing and adult brain, with highest levels observed in the cerebellum and cerebral cortex.[28] The protein binds to voltage-gated Na^+ (NaV) channels and promotes their localization to the proximal region of the axon, providing the fine-tuned regulation necessary for normal functioning.[37,38] The development of ataxia and paroxysmal dyskinesia in mice lacking *Fgf14* was the first direct evidence potentially linking the gene to human disease.[39] Notably, FGF14 is required for spontaneous and evoked firing in cerebellar Purkinje neurons and for motor co-ordination and balance.[40,41] Therefore, although our functional studies of primary fibroblasts were inconclusive, we hypothesize that the pathogenic mechanism underlying *FGF14* $(GAA)_n$-mediated ataxia is reduced functional protein due to decreased expression of the allele with the RE. Such a mechanism is somewhat analogous to Friedreich ataxia, the only other known example of an ataxia mediated by a $(GAA)_n$ RE. This mechanism is also consistent with our observation that GAAGGA repeats, such as $(GAAGGA)_{166}$, equivalent in size to $(GAA)_{332}$, are not associated with ataxia (Figure 3). GGA interruptions in long GAA repeats have been shown to inhibit the formation of triplex and sticky DNA structures and alleviate transcription inhibition.[42] However, additional functional studies will be required to test the haploinsufficiency hypothesis. This could be achieved by direct analysis of FGF14 mRNA expression and/or steady-state protein level in postmortem brain from individuals with a pathogenic expanded repeat. Alternatively, generating and analyzing neurons differentiated from proband-derived iPSCs would likely be informative regarding the effect of the GAA expansion on *FGF14* expression.

Our proposed genotype-phenotype correlation is consistent with the observation that point mutations and other non-RE genetic variants in *FGF14* cause autosomal-dominant cerebellar ataxia (SCA27, also known as ATX-FGF14).[24,43] The underlying pathogenic mechanism in SCA27 is a 50% reduction in the normal level of functional protein, i.e., haploinsufficiency. SCA27 is a rare form of inherited CA and is described in fewer than 30 families.[44] Affected individuals tend to present with early-onset CA associated with widespread tremors, dyskinesias, significant cognitive impairment, and psychiatric features,[24,45,46] the latter potentially severe.[47] Less commonly reported signs are microcephaly, clinodactyly, and pes cavus.[43] In contrast, people with *FGF14* $(GAA)_n$-mediated ataxia present at a later age with a less severe disease course, outcomes predicted by a reduction but not complete loss of expression of the mutant *FGF14* allele. A similar genotype-phenotype correlation occurs with *CACNA1A*: heterozygous point mutations are associated with episodic ataxia (EA2 [MIM: 108500]), which almost exclusively manifests prior to 20 years of age whereas a $(CAG)_n$ RE in the gene is associated with an adult-onset, slowly progressive spinocerebellar ataxia (SCA6 [MIM: 183086]).[48]

The core phenotypes associated with *FGF14* $(GAA)_n$-mediated ataxia are pure CA and cerebellar ataxia with bilateral vestibulopathy (CABV), with the variable presence of other features including hyper-reflexia and autonomic dysfunction. Notably, both CA and CABV are conspicuously under-represented in individuals with ataxia in whom a genetic diagnosis is achieved. For example, they are rarely observed in *RFC1*-mediated disease,[49,50] which is thought to be the most common inherited cause of CA.[51] The identification and high prevalence of *FGF14* $(GAA)_n$-mediated ataxia, a novel RE

mutation mechanism in a gene previously known to cause a related phenotype, may account for a significant proportion of unresolved individuals with ataxia and fill this diagnostic vacuum. A noteworthy feature of our study is that several participants partially fulfilled criteria for CANVAS with cerebellar ataxia and vestibulopathy, some with additional cough and autonomic failure but all lacking large fiber sensory neuropathy. Our identification of a *FGF14* $(GAA)_n$ RE in these patients provides an alternative genetic cause in individuals with CANVAS-like syndromes negative for bi-allelic *RFC1* RE. A feature of other RE-mediated CAs such as SCA1,2,3,6,7[52] and Friedreich ataxia[53] is an inverse relationship between repeat length and age at disease onset. Identifying such a relationship can aid prognostication; for example, in Machado-Joseph disease (SCA3 [MIM: 607047]), larger expansions are also associated with a more rapid disease progression and varying phenotypes.[6] Despite the relatively small cohort sizes, we identified a negative correlation between age at onset and repeat length ($R^2 = 0.44$, $p = 0.00045$, slope $= -0.12$, Figure S8).

In conclusion, we show that a heterozygous $(GAA)_n$ RE located in intron 1 of *FGF14* is a common cause of adult-onset ataxia, in particular individuals with pure CA or CABV phenotypes, a cohort in whom genetic diagnosis is relatively rarely forthcoming. Consistent with the nomenclature guidelines widely utilized by clinicians, we propose the name SCA50 for this newly described disorder. In accordance with the guidelines established by the Movement Disorder Society Task Force for genetic movement disorders[54,55] the nomenclature for this ataxia is ATX-FGF14. Our data suggest that $(GAA)_{>250}$ be considered as pathogenic, with acknowledgment of potential incomplete penetrance. It is not currently possible to define an upper size whereby expansions might be classified as fully penetrant, but our analysis of >500 control subjects suggests $(GAA)_{>335}$. Generating more specific pathogenic ranges will require analysis of large cohorts and families. In addition, given that both size and composition appear to be key mediators of pathogenicity, fully resolving these key questions will require application of advanced sequencing technologies, in addition to more traditional molecular tools such as LR-PCR and RP-PCR. Notably, despite the advances in RE diagnostics being enabled by short-read genome sequencing,[56] this study highlights limitations of short-read data and bioinformatic tools such as ExpansionHunter and exSTRa to interrogate the structure of the $(GAA)_n$ RE and the difficulty in interrogating larger REs (>150 bp). Application of multiple bioinformatic tools, including EHDN, in combination with long-read sequencing technologies will be required to unravel the full genotype-phenotype relationships in SCA50.

Data and code availability

The accession for the *FGF14* variants reported in this paper is ClinVar: SCV002576522. The datasets and code supporting the current study are available at the links described in web resources. Sequencing data have not been deposited in a public repository due to restrictions associated with participant consent but are available from the corresponding author on reasonable and appropriate request.

Supplemental information

Supplemental information can be found online at https://doi.org/10.1016/j.ajhg.2022.11.015.

Acknowledgments

This work was supported by the Australian Government National Health and Medical Research Council grants (GNT2001513 and MRFF2007677) to P.J.L., M.B.D., and H.R. H.R. was supported by an NHMRC Emerging Leadership 1 grant (1194364) and M.B. was supported by an NHMRC Leadership 1 grant (1195236). Additional funding was provided by the Independent Research Institute Infrastructure Support Scheme, the Victorian State Government Operational Infrastructure Program and the Murdoch Children's Research Institute. N.B. and K.L. are supported by research grants from the Deutsche Forschungsgemeinschaft (DFG, FOR 2488). We would like to thank Frauke Hinrichs for technical support and Christoph Helmchen, Max Borsche, and Meike Kasten for help with the recruitment of the German participants.

Declaration of interests

The authors declare no competing interests.

Received: October 12, 2022
Accepted: November 19, 2022
Published: December 8, 2022

Web resources

Cavalier, https://github.com/bahlolab/nf-cavalier
ClinVar, https://www.ncbi.nlm.nih.gov/clinvar/
curated ataxia gene list, https://doi.org/10.5281/zenodo.7317517
dbSNP-ALFA, https://www.ncbi.nlm.nih.gov/snp/docs/gsr/alfa/
exSTRa, https://github.com/bahlolab/exSTRa/blob/abdf75d89f095f7b7f8573d22206edd735d8914b/inst/extdata/repeat_expansion_disorders_hg38.txt
Genotype-Tissue Expression (GTEx) project, https://gtexportal.org/home/
Genome Aggregation Database (gnomAD), http://gnomad.broadinstitute.org/
Integrative Genomics Viewer (IGV), http://software.broadinstitute.org/software/igv/
Online Mendelian Inheritance in Man, http://www.omim.org/
PanelApp Australia, https://panelapp.agha.umccr.org/
PanelApp UK, https://panelapp.genomicsengland.co.uk/
UCSC Genome Bioinformatics database, https://genome.ucsc.edu/
Varsome, https://varsome.com

References

1. Ruano, L., Melo, C., Silva, M.C., and Coutinho, P. (2014). The global epidemiology of hereditary ataxia and spastic paraplegia: a systematic review of prevalence studies.

Neuroepidemiology *42*, 174–183. https://doi.org/10.1159/000358801.
2. Benson, G. (1999). Tandem repeats finder: a program to analyze DNA sequences. Nucleic Acids Res. *27*, 573–580.
3. Mousavi, N., Shleizer-Burko, S., Yanicky, R., and Gymrek, M. (2019). Profiling the genome-wide landscape of tandem repeat expansions. Nucleic Acids Res. *47*, e90. https://doi.org/10.1093/nar/gkz501.
4. Depienne, C., and Mandel, J.L. (2021). 30 years of repeat expansion disorders: what have we learned and what are the remaining challenges? Am. J. Hum. Genet. *108*, 764–785. https://doi.org/10.1016/j.ajhg.2021.03.011.
5. Harding, A.E. (1981). Idiopathic" late onset cerebellar ataxia. A clinical and genetic study of 36 cases. J. Neurol. Sci. *51*, 259–271.
6. Klockgether, T., Kramer, B., Lüdtke, R., Schöls, L., and Laccone, F. (1996). Repeat length and disease progression in spinocerebellar ataxia type 3. Lancet *348*, 830. https://doi.org/10.1016/S0140-6736(05)65255-5.
7. Rexach, J., Lee, H., Martinez-Agosto, J.A., Németh, A.H., and Fogel, B.L. (2019). Clinical application of next-generation sequencing to the practice of neurology. Lancet Neurol. *18*, 492–503. https://doi.org/10.1016/S1474-4422(19)30033-X.
8. Bahlo, M., Bennett, M.F., Degorski, P., Tankard, R.M., Delatycki, M.B., and Lockhart, P.J. (2018). Recent advances in the detection of repeat expansions with short-read next-generation sequencing. F1000Res. *7*, 736. https://doi.org/10.12688/f1000research.13980.1.
9. Dolzhenko, E., Bennett, M.F., Richmond, P.A., Trost, B., Chen, S., van Vugt, J.J.F.A., Nguyen, C., Narzisi, G., Gainullin, V.G., Gross, A.M., et al. (2020). ExpansionHunter Denovo: a computational method for locating known and novel repeat expansions in short-read sequencing data. Genome Biol. *21*, 102. https://doi.org/10.1186/s13059-020-02017-z.
10. Rafehi, H., Szmulewicz, D.J., Bennett, M.F., Sobreira, N.L.M., Pope, K., Smith, K.R., Gillies, G., Diakumis, P., Dolzhenko, E., Eberle, M.A., et al. (2019). Bioinformatics-based identification of expanded repeats: a non-reference intronic pentamer expansion in RFC1 causes CANVAS. Am. J. Hum. Genet. *105*, 151–165. https://doi.org/10.1016/j.ajhg.2019.05.016.
11. Payne, A., Holmes, N., Clarke, T., Munro, R., Debebe, B.J., and Loose, M. (2021). Readfish enables targeted nanopore sequencing of gigabase-sized genomes. Nat. Biotechnol. *39*, 442–450. https://doi.org/10.1038/s41587-020-00746-x.
12. DePristo, M.A., Banks, E., Poplin, R., Garimella, K.V., Maguire, J.R., Hartl, C., Philippakis, A.A., del Angel, G., Rivas, M.A., Hanna, M., et al. (2011). A framework for variation discovery and genotyping using next-generation DNA sequencing data. Nat. Genet. *43*, 491–498. https://doi.org/10.1038/ng.806.
13. Auwera, G.A., Carneiro, M.O., Hartl, C., Poplin, R., Del Angel, G., Levy-Moonshine, A., Jordan, T., Shakir, K., Roazen, D., Thibault, J., et al. (2013). From FastQ data to high confidence variant calls: the Genome Analysis Toolkit best practices pipeline. Curr. Protoc. Bioinformatics *43*. 11 10 11-11 10 33. https://doi.org/10.1002/0471250953.bi1110s43.
14. Tankard, R.M., Bennett, M.F., Degorski, P., Delatycki, M.B., Lockhart, P.J., and Bahlo, M. (2018). Detecting expansions of tandem repeats in cohorts sequenced with short-read sequencing data. Am. J. Hum. Genet. *103*, 858–873. https://doi.org/10.1016/j.ajhg.2018.10.015.
15. Dolzhenko, E., Deshpande, V., Schlesinger, F., Krusche, P., Petrovski, R., Chen, S., Emig-Agius, D., Gross, A., Narzisi, G., Bowman, B., et al. (2019). ExpansionHunter: a sequence-graph-based tool to analyze variation in short tandem repeat regions. Bioinformatics *35*, 4754–4756. https://doi.org/10.1093/bioinformatics/btz431.
16. 1000 Genomes Project Consortium, Auton, A., Brooks, L.D., Durbin, R.M., Garrison, E.P., Kang, H.M., Korbel, J.O., Marchini, J.L., McCarthy, S., McVean, G.A., and Abecasis, G.R. (2015). A global reference for human genetic variation. Nature *526*, 68–74. https://doi.org/10.1038/nature15393.
17. Byrska-Bishop, M., Evani, U.S., Zhao, X., Basile, A.O., Abel, H.J., Regier, A.A., Corvelo, A., Clarke, W.E., Musunuri, R., Nagulapalli, K., et al. (2022). High-coverage whole-genome sequencing of the expanded 1000 Genomes Project cohort including 602 trios. Cell *185*, 3426–3440.e19. https://doi.org/10.1016/j.cell.2022.08.004.
18. Di Tommaso, P., Chatzou, M., Floden, E.W., Barja, P.P., Palumbo, E., and Notredame, C. (2017). Nextflow enables reproducible computational workflows. Nat. Biotechnol. *35*, 316–319. https://doi.org/10.1038/nbt.3820.
19. McKenna, A., Hanna, M., Banks, E., Sivachenko, A., Cibulskis, K., Kernytsky, A., Garimella, K., Altshuler, D., Gabriel, S., Daly, M., and DePristo, M.A. (2010). The Genome Analysis Toolkit: a MapReduce framework for analyzing next-generation DNA sequencing data. Genome Res. *20*, 1297–1303. https://doi.org/10.1101/gr.107524.110.
20. Li, H. (2011). A statistical framework for SNP calling, mutation discovery, association mapping and population genetical parameter estimation from sequencing data. Bioinformatics *27*, 2987–2993. https://doi.org/10.1093/bioinformatics/btr509.
21. Robinson, J.T., Thorvaldsdóttir, H., Winckler, W., Guttman, M., Lander, E.S., Getz, G., and Mesirov, J.P. (2011). Integrative genomics viewer. Nat. Biotechnol. *29*, 24–26. https://doi.org/10.1038/nbt.1754.
22. McLaren, W., Gil, L., Hunt, S.E., Riat, H.S., Ritchie, G.R.S., Thormann, A., Flicek, P., and Cunningham, F. (2016). The Ensembl Variant Effect Predictor. Genome Biol. *17*, 122. https://doi.org/10.1186/s13059-016-0974-4.
23. Mitsuhashi, S., Frith, M.C., Mizuguchi, T., Miyatake, S., Toyota, T., Adachi, H., Oma, Y., Kino, Y., Mitsuhashi, H., and Matsumoto, N. (2019). Tandem-genotypes: robust detection of tandem repeat expansions from long DNA reads. Genome Biol. *20*, 58. https://doi.org/10.1186/s13059-019-1667-6.
24. van Swieten, J.C., Brusse, E., de Graaf, B.M., Krieger, E., van de Graaf, R., de Koning, I., Maat-Kievit, A., Leegwater, P., Dooijes, D., Oostra, B.A., and Heutink, P. (2003). A mutation in the fibroblast growth factor 14 gene is associated with autosomal dominant cerebellar ataxia [corrected]. Am. J. Hum. Genet. *72*, 191–199. https://doi.org/10.1086/345488.
25. Zühlke, C., Dalski, A., Hellenbroich, Y., Bubel, S., Schwinger, E., and Bürk, K. (2002). Spinocerebellar ataxia type 1 (SCA1): phenotype-genotype correlation studies in intermediate alleles. Eur. J. Hum. Genet. *10*, 204–209. https://doi.org/10.1038/sj.ejhg.5200788.
26. Menon, R.P., Nethisinghe, S., Faggiano, S., Vannocci, T., Rezaei, H., Pemble, S., Sweeney, M.G., Wood, N.W., Davis, M.B., Pastore, A., and Giunti, P. (2013). The role of interruptions in polyQ in the pathology of SCA1. PLoS Genet. *9*, e1003648. https://doi.org/10.1371/journal.pgen.1003648.
27. Pearson, C.E., Eichler, E.E., Lorenzetti, D., Kramer, S.F., Zoghbi, H.Y., Nelson, D.L., and Sinden, R.R. (1998). Interruptions in the triplet repeats of SCA1 and FRAXA reduce the

propensity and complexity of slipped strand DNA (S-DNA) formation. Biochemistry *37*, 2701–2708. https://doi.org/10.1021/bi972546c.

28. Wang, Q., McEwen, D.G., and Ornitz, D.M. (2000). Subcellular and developmental expression of alternatively spliced forms of fibroblast growth factor 14. Mech. Dev. *90*, 283–287. https://doi.org/10.1016/s0925-4773(99)00241-5.
29. Bidichandani, S.I., Ashizawa, T., and Patel, P.I. (1998). The GAA triplet-repeat expansion in Friedreich ataxia interferes with transcription and may be associated with an unusual DNA structure. Am. J. Hum. Genet. *62*, 111–121. https://doi.org/10.1086/301680.
30. Kuhlmann, K., Cieselski, M., and Schumann, J. (2021). Relative versus absolute RNA quantification: a comparative analysis based on the example of endothelial expression of vasoactive receptors. Biol. Proced. Online *23*, 6. https://doi.org/10.1186/s12575-021-00144-w.
31. MacDougall, H.G., Weber, K.P., McGarvie, L.A., Halmagyi, G.M., and Curthoys, I.S. (2009). The video head impulse test: diagnostic accuracy in peripheral vestibulopathy. Neurology *73*, 1134–1141. https://doi.org/10.1212/WNL.0b013e3181bacf85.
32. Szmulewicz, D., MacDougall, H., Storey, E., Curthoys, I., and Halmagyi, M. (2014). A novel quantitative bedside test of balance function: the video visually enhanced vestibulo-ocular reflex (VVOR). Neurology *82*, S19–S1002.
33. Paulson, H. (2018). Repeat expansion diseases. Handb. Clin. Neurol. *147*, 105–123. https://doi.org/10.1016/B978-0-444-63233-3.00009-9.
34. Ibañez, K., Polke, J., Hagelstrom, R.T., Dolzhenko, E., Pasko, D., Thomas, E.R.A., Daugherty, L.C., Kasperaviciute, D., Smith, K.R., et al.; WGS for Neurological Diseases Group (2022). Whole genome sequencing for the diagnosis of neurological repeat expansion disorders in the UK: a retrospective diagnostic accuracy and prospective clinical validation study. Lancet Neurol. *21*, 234–245. https://doi.org/10.1016/S1474-4422(21)00462-2.
35. Strupp, M., Maul, S., Konte, B., Hartmann, A.M., Giegling, I., Wollenteit, S., Feil, K., and Rujescu, D. (2020). A variation in FGF14 is associated with downbeat nystagmus in a genome-wide association study. Cerebellum *19*, 348–357. https://doi.org/10.1007/s12311-020-01113-x.
36. Wagner, J.N., Glaser, M., Brandt, T., and Strupp, M. (2008). Downbeat nystagmus: aetiology and comorbidity in 117 patients. J. Neurol. Neurosurg. Psychiatry *79*, 672–677. https://doi.org/10.1136/jnnp.2007.126284.
37. Lou, J.Y., Laezza, F., Gerber, B.R., Xiao, M., Yamada, K.A., Hartmann, H., Craig, A.M., Nerbonne, J.M., and Ornitz, D.M. (2005). Fibroblast growth factor 14 is an intracellular modulator of voltage-gated sodium channels. J. Physiol. *569*, 179–193. https://doi.org/10.1113/jphysiol.2005.097220.
38. Di Re, J., Wadsworth, P.A., and Laezza, F. (2017). Intracellular fibroblast growth factor 14: emerging risk factor for brain disorders. Front. Cell. Neurosci. *11*, 103. https://doi.org/10.3389/fncel.2017.00103.
39. Wang, Q., Bardgett, M.E., Wong, M., Wozniak, D.F., Lou, J., McNeil, B.D., Chen, C., Nardi, A., Reid, D.C., Yamada, K., and Ornitz, D.M. (2002). Ataxia and paroxysmal dyskinesia in mice lacking axonally transported FGF14. Neuron *35*, 25–38. https://doi.org/10.1016/s0896-6273(02)00744-4.
40. Bosch, M.K., Carrasquillo, Y., Ransdell, J.L., Kanakamedala, A., Ornitz, D.M., and Nerbonne, J.M. (2015). Intracellular FGF14 (iFGF14) is required for spontaneous and evoked firing in cerebellar purkinje neurons and for motor coordination and balance. J. Neurosci. *35*, 6752–6769. https://doi.org/10.1523/JNEUROSCI.2663-14.2015.
41. Yan, H., Pablo, J.L., Wang, C., and Pitt, G.S. (2014). FGF14 modulates resurgent sodium current in mouse cerebellar Purkinje neurons. Elife *3*, e04193. https://doi.org/10.7554/eLife.04193.
42. Sakamoto, N., Larson, J.E., Iyer, R.R., Montermini, L., Pandolfo, M., and Wells, R.D. (2001). GGA*TCC-interrupted triplets in long GAA*TTC repeats inhibit the formation of triplex and sticky DNA structures, alleviate transcription inhibition, and reduce genetic instabilities. J. Biol. Chem. *276*, 27178–27187. https://doi.org/10.1074/jbc.M101852200.
43. Misceo, D., Fannemel, M., Barøy, T., Roberto, R., Tvedt, B., Jaeger, T., Bryn, V., Strømme, P., and Frengen, E. (2009). SCA27 caused by a chromosome translocation: further delineation of the phenotype. Neurogenetics *10*, 371–374. https://doi.org/10.1007/s10048-009-0197-x.
44. Groth, C.L., and Berman, B.D. (2018). Spinocerebellar ataxia 27: a review and characterization of an evolving phenotype. Tremor Other Hyperkinet. Mov. *8*, 534. https://doi.org/10.7916/D80S0ZJQ.
45. Dalski, A., Atici, J., Kreuz, F.R., Hellenbroich, Y., Schwinger, E., and Zühlke, C. (2005). Mutation analysis in the fibroblast growth factor 14 gene: frameshift mutation and polymorphisms in patients with inherited ataxias. Eur. J. Hum. Genet. *13*, 118–120. https://doi.org/10.1038/sj.ejhg.5201286.
46. Miura, S., Kosaka, K., Fujioka, R., Uchiyama, Y., Shimojo, T., Morikawa, T., Irie, A., Taniwaki, T., and Shibata, H. (2019). Spinocerebellar ataxia 27 with a novel nonsense variant (Lys177X) in FGF14. Eur. J. Med. Genet. *62*, 172–176. https://doi.org/10.1016/j.ejmg.2018.07.005.
47. Paucar, M., Lundin, J., Alshammari, T., Bergendal, Å., Lindefeldt, M., Alshammari, M., Solders, G., Di Re, J., Savitcheva, I., Granberg, T., et al. (2020). Broader phenotypic traits and widespread brain hypometabolism in spinocerebellar ataxia 27. J. Intern. Med. *288*, 103–115. https://doi.org/10.1111/joim.13052.
48. Casey, H.L., and Gomez, C.M. (1993). Spinocerebellar ataxia type 6. GeneReviews. https://www.ncbi.nlm.nih.gov/books/NBK1140/.
49. Gisatulin, M., Dobricic, V., Zühlke, C., Hellenbroich, Y., Tadic, V., Münchau, A., Isenhardt, K., Bürk, K., Bahlo, M., Lockhart, P.J., et al. (2020). Clinical spectrum of the pentanucleotide repeat expansion in the RFC1 gene in ataxia syndromes. Neurology *95*, e2912–e2923. https://doi.org/10.1212/WNL.0000000000010744.
50. Montaut, S., Diedhiou, N., Fahrer, P., Marelli, C., Lhermitte, B., Robelin, L., Vincent, M.C., Corti, L., Taieb, G., Gebus, O., et al. (2021). Biallelic RFC1-expansion in a French multicentric sporadic ataxia cohort. J. Neurol. *268*, 3337–3343. https://doi.org/10.1007/s00415-021-10499-5.
51. Davies, K., Szmulewicz, D.J., Corben, L.A., Delatycki, M., and Lockhart, P.J. (2022). RFC1-related disease: molecular and clinical insights. Neurol. Genet. *8*, e200016. https://doi.org/10.1212/NXG.0000000000200016.
52. Tezenas du Montcel, S., Durr, A., Bauer, P., Figueroa, K.P., Ichikawa, Y., Brussino, A., Forlani, S., Rakowicz, M., Schöls, L., Mariotti, C., et al. (2014). Modulation of the age at onset in spinocerebellar ataxia by CAG tracts in various genes. Brain *137*, 2444–2455. https://doi.org/10.1093/brain/awu174.

53. Delatycki, M.B., Williamson, R., and Forrest, S.M. (2000). Friedreich ataxia: an overview. J. Med. Genet. *37*, 1–8. https://doi.org/10.1136/jmg.37.1.1.
54. Lange, L.M., Gonzalez-Latapi, P., Rajalingam, R., Tijssen, M.A.J., Ebrahimi-Fakhari, D., Gabbert, C., Ganos, C., Ghosh, R., Kumar, K.R., Lang, A.E., et al. (2022). Nomenclature of genetic movement disorders: recommendations of the international parkinson and movement disorder society task force - an update. Mov. Disord. *37*, 905–935. https://doi.org/10.1002/mds.28982.
55. Marras, C., Lang, A., van de Warrenburg, B.P., Sue, C.M., Tabrizi, S.J., Bertram, L., Mercimek-Mahmutoglu, S., Ebrahimi-Fakhari, D., Warner, T.T., Durr, A., et al. (2016). Nomenclature of genetic movement disorders: Recommendations of the international Parkinson and movement disorder society task force. Mov. Disord. *31*, 436–457. https://doi.org/10.1002/mds.26527.
56. Lockhart, P.J. (2022). Advancing the diagnosis of repeat expansion disorders. Lancet Neurol. *21*, 205–207. https://doi.org/10.1016/S1474-4422(22)00033-3.

The American Journal of Human Genetics, Volume *110*

Supplemental information

An intronic GAA repeat expansion in *FGF14* causes the autosomal-dominant adult-onset ataxia SCA50/ATX-FGF14

Haloom Rafehi, Justin Read, David J. Szmulewicz, Kayli C. Davies, Penny Snell, Liam G. Fearnley, Liam Scott, Mirja Thomsen, Greta Gillies, Kate Pope, Mark F. Bennett, Jacob E. Munro, Kathie J. Ngo, Luke Chen, Mathew J. Wallis, Ernest G. Butler, Kishore R. Kumar, Kathy HC. Wu, Susan E. Tomlinson, Stephen Tisch, Abhishek Malhotra, Matthew Lee-Archer, Egor Dolzhenko, Michael A. Eberle, Leslie J. Roberts, Brent L. Fogel, Norbert Brüggemann, Katja Lohmann, Martin B. Delatycki, Melanie Bahlo, and Paul J. Lockhart

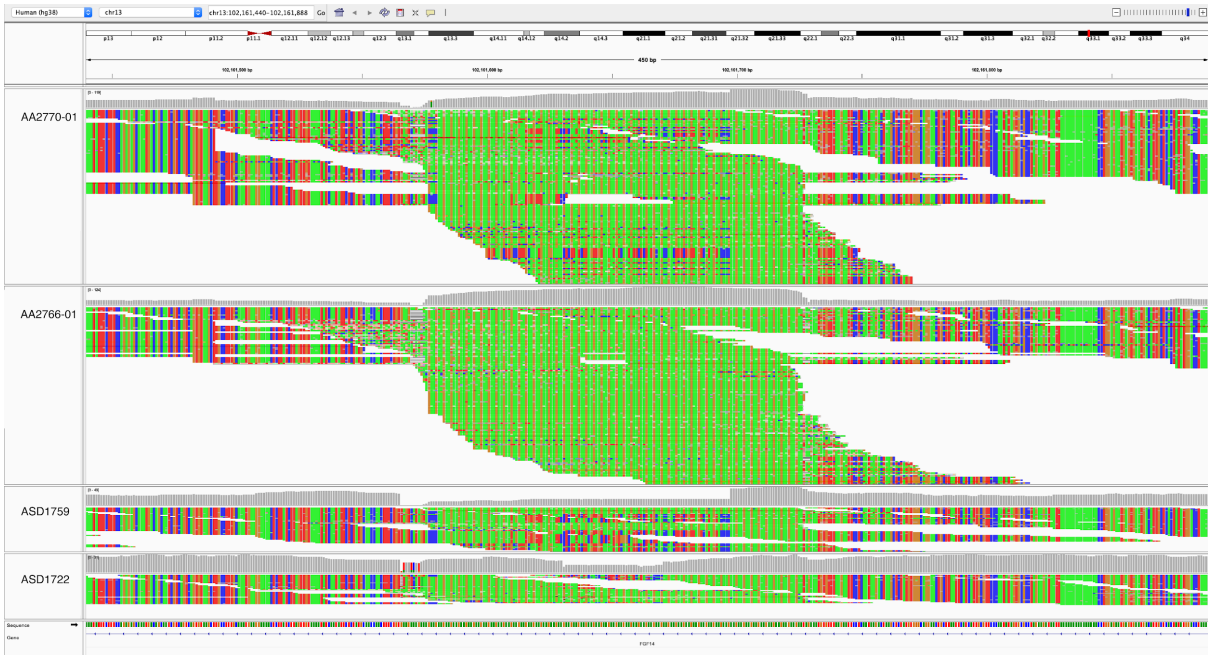

Figure S1: IGV snapshots of the $(GAA)_n$ locus in *FGF14*.

Visualization of the GS reads in IGV for individuals with an expanded (GAA) RE (top two images) compared to controls (bottom two images).

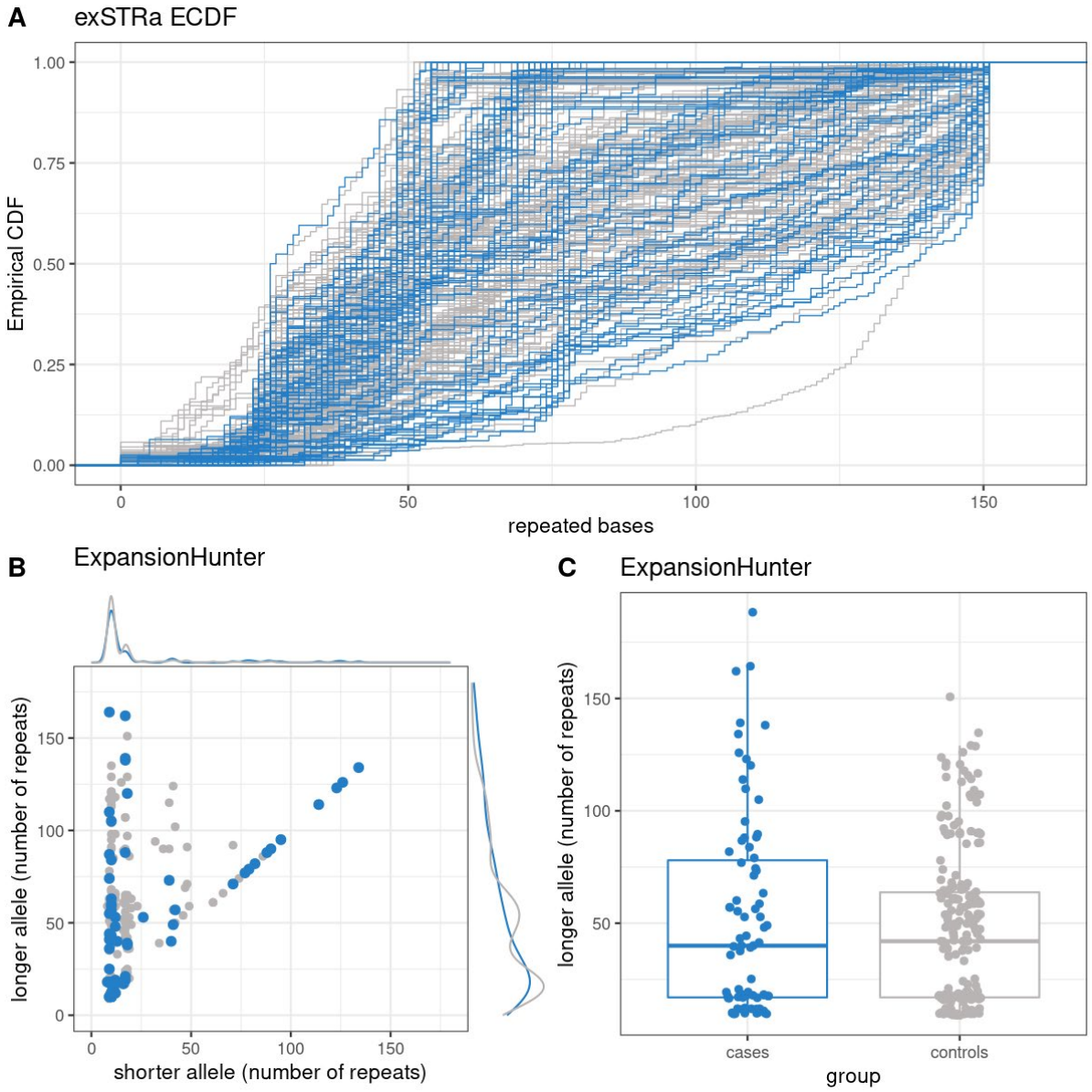

Figure S2: Plots of exSTRa and ExpansionHunter outputs for the *FGF14* (GAA) locus

The *FGF14* (GAA) STR was profiled in cases (blue) and controls (grey) using bioinformatics tools, showing inability of bioinformatic tools to accurately estimate the size of the *FGF14* STR, particularly for alleles with $>(GAA)_{100}$. (A) exSTRa ECDF plot fails to distinguish outliers, due to the high variability of and large size of the STR in the general population. (B) Size estimates of the *FGF14* (GAA) STR were determined using ExpansionHunter. Density plots are show the allele repeat distributions for cases (blue) and controls (grey) for the longer (y-axis) and shorter (x-axis) alleles. (C) Comparison of longer allele size determined by ExpansionHunter in cases versus controls.

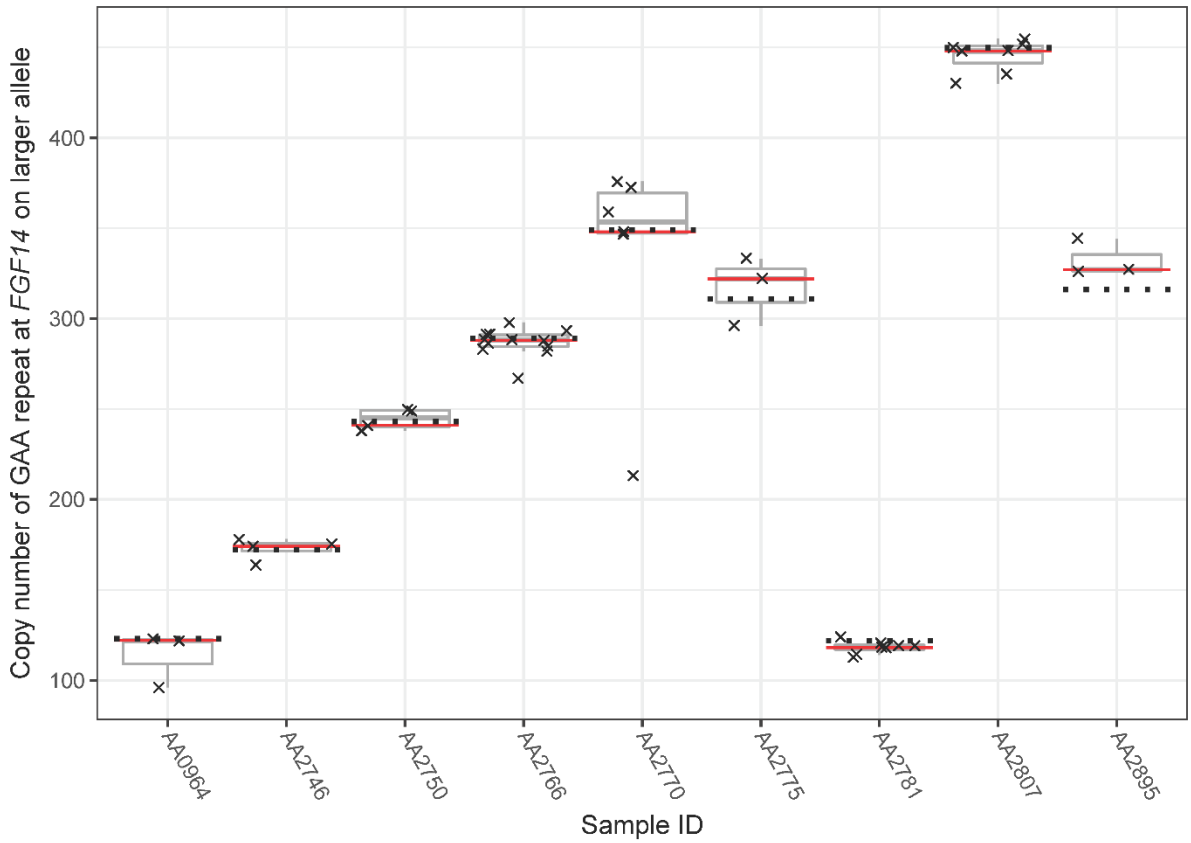

Figure S3: Nanopore repeat size estimates concur with PCR estimates. Eight probands were sequenced with Oxford Nanopore MinION adaptive sequencing targeting *FGF14*. The $(GAA)_n$ repeat was genotyped in the long-read sequencing data using tandem-genotypes. Repeat sizes from Nanopore sequencing are shown for each read (crosses) and as a distribution (box plot), along with the tandem-genotypes (red line) and PCR (dotted line) size estimates for each sample. All samples except AA0964, AA2764 and AA2781 encoded a pathogenic *FGF14* allele.

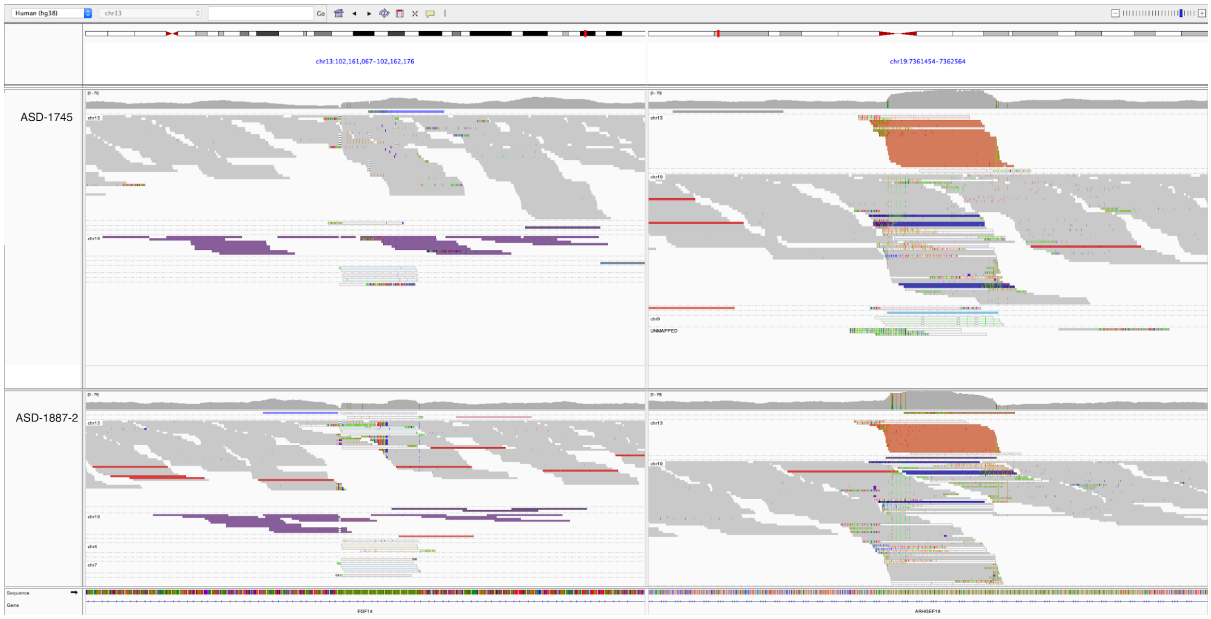

SF4: IGV snapshot of controls with unusual RP-PCR patterns

Visualization of the genome sequence reads in IGV for controls with an expanded GAAGGA RE at the *FGF14* $(GAA)_n$ STR (left panel). Reads coloured in purple uniquely map to the *FGF14* locus, however their read pairs map to a GAAGGA motif in another region of the genome (right panel, reads in orange).

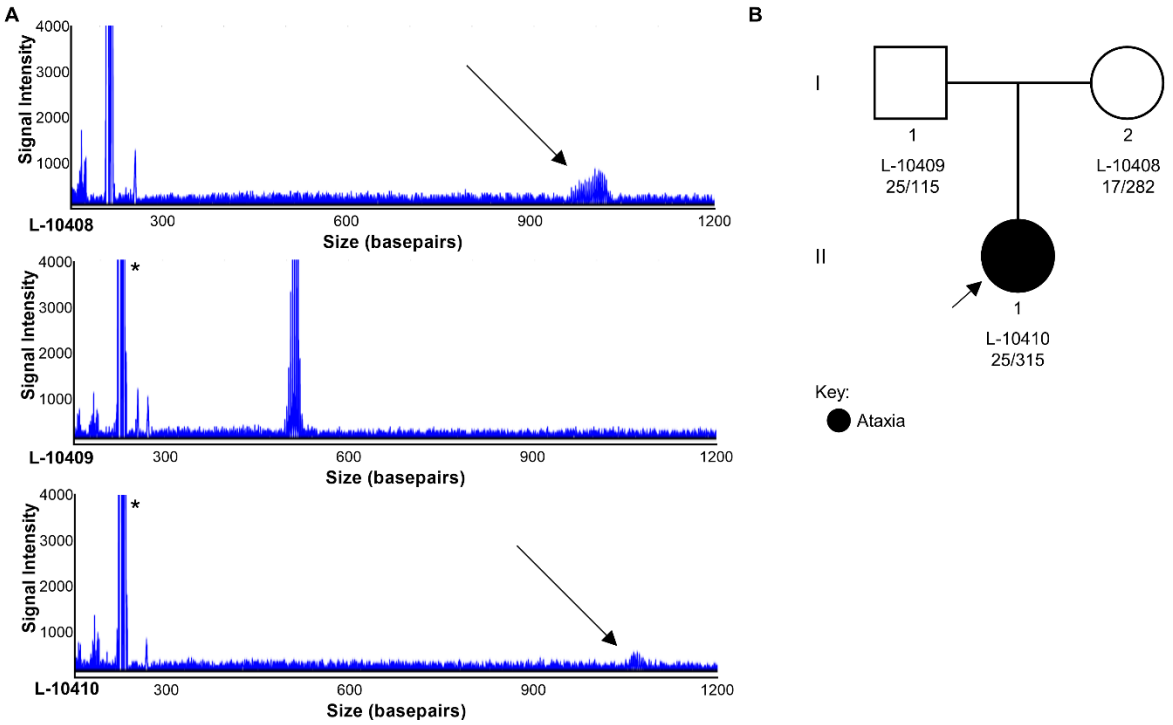

Figure S5: Intergenerational expansion of *FGF14* (GAA)n STR

LR-PCR electropherograms of *FGF14* STR by capillary array (A) for II-1 (L-10410) and unaffected parents (L-10408 and L-10409) (B). Allele sizing for L-10408 at this locus demonstrated that the paternal allele $(GAA)_{25}$ (indicated by *) was inherited unchanged, whereas the maternal allele increased from $(GAA)_{282}$ to $(GAA)_{315}$ in the affected daughter.

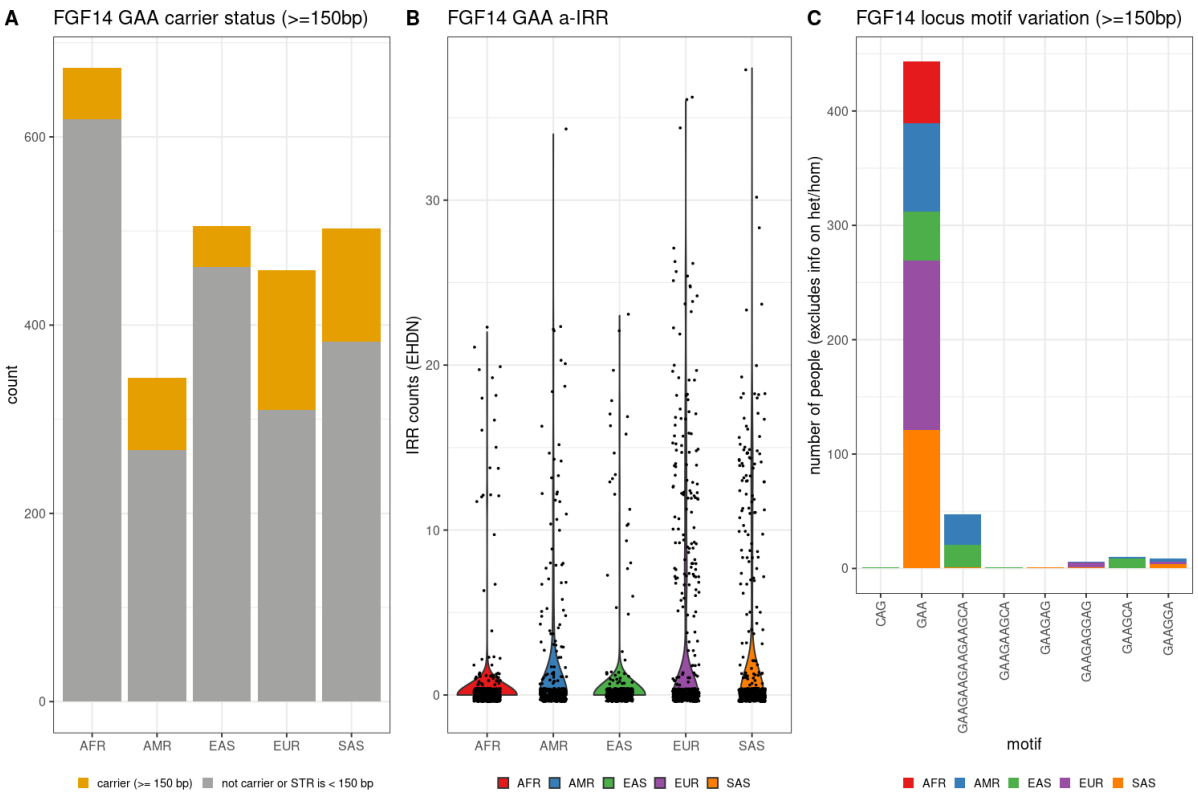

Figure S6: Profiling the *FGF14* (GAA) RE locus in the 1000 Genomes Project.
The *FGF14* (GAA) STR locus was profiled in 2483 unrelated individuals from the 1000 Genomes Project from African (AFR), ad mixed American (AMR), East Asian (EAS), European (EUR) and South Asian (SAS) populations. (A) Number of *FGF14* (GAA) STR carriers in the 1000 Genomes Project, by ethnicity. Carriers are defined as having an STR >= 150 bp (or 50 repeats). (B) Violin plot showing the distribution of the a-IRR for the *FGF14* (GAA) STR by ethnicity. Individuals without a reported a-IRR, either because they do not carry the STR, or they carry the STR with <150 bp (or 50 repeats), are coded as zero. (C) Bar chart showing the alternative motifs also detected at the *FGF14* (GAA) locus, split by ethnicity. Only motifs present at >= 150bp in at least one individual are reported.

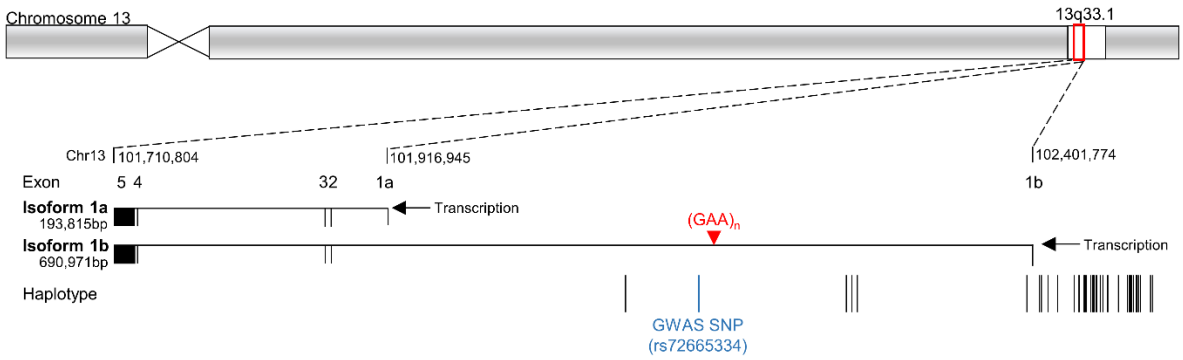

Figure S7. *FGF14* genomic region, haplotype and isoform structure

Schematic representation of the chromosomal location of *FGF14* to 13q33.1, illustrating the expression sites of two mRNA isoforms, 1a and 1b. Exon one of isoform 1b is located 5' of 1a, and the $(GAA)_n$ STR is located within the intervening intron. The remaining exons 2-5, are common to both isoforms. The SNP (rs72665334) identified by GWAS to be associated with down beat nystagmus is located ~10kb 3' of the $(GAA)_n$ STR. A common ancestral haplotype was determined for three Australian cases with $(GAA)_{>250}$ by comparing variant sharing around the *FGF14* STR (gnomAD AF<0.1) (specific haplotype details in Table S3).

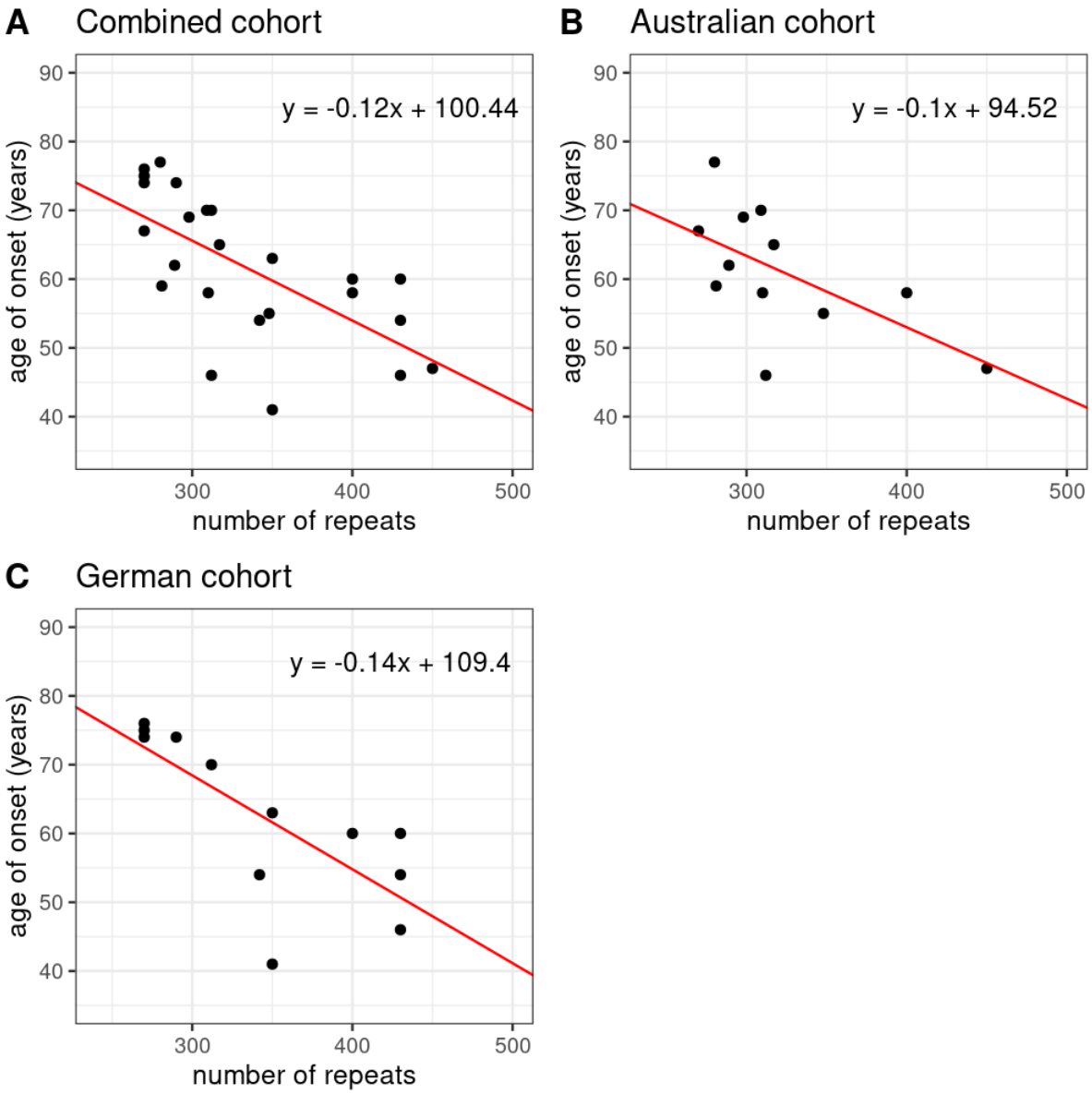

Figure S8: Linear regression comparing *FGF14* $(GAA)_n$ RE number of repeats and age at onset.

A linear regression was used to determine the relationship between ataxia age at onset and *FGF14* $(GAA)_n$ repeat length for the (A) combined (n=24), (B) Australian (n=12) and (C) German (n=12) cohorts. Repeat lengths were determined using LR-PCR. Individuals with ataxia of known age at onset with $(GAA)_{>250}$ were included in the analysis.

Table S1: Primer sequences for analysis of *FGF14*.

Primer name	Position (hg38)	Sequence
FGF14_RPP_ F1	chr13:102161468-102161490	5'-AGCAATCGTCAGTCAGTGTAAGC
FGF14_LRP_ R1	chr13:102161762-102161782	5'-CAGTTCCTGCCCACATAGAGC
FGF14_RPP_ F1_FAM	chr13:102161468-102161490	FAM-5'-AGCAATCGTCAGTCAGTGTAAGC
FGF14_RPP_AAG_RE_R1	NA	5'-CAGGAAACAGCTATGACC CTTCTTCTTCTTCTTCTTCTT
RPP_M13R	NA	5'-CAGGAAACAGCTATGACC

The gene reference sequences utilized for *FGF14* were NC_000013.11, NM_004115.4 (Isoform 1a) and NM_175929.3 (Isoform 1b).

Table S2. *FGF14* allele sizing for individuals with $(GAA)_{>250}$ in Australian and German cohorts

Australian Cohort						
Affected Individuals			Controls			
Alias	Allele		Alias	Age (years)	Allele	
	1	2			1	2
AA2807	170	450	ASD1745	48	65	332*
AA2831	74	400	C0063	61	12	300
AA2903	19	400	ASD1808	43	12	296*
AA2770	13	349	ASD1887	38	22	282*
AA2895	58	316	C0090	46	12	270
AA0441	19	315				
AA2809	12	313				
AA2775	57	311				
AA2845	19	296				
AA2766	185	289				
AA2933	20	284				
AA2926	12	268				
AA2908	14	256				

German Validation Cohort						
Affected Individuals			Controls			
Alias	Allele		Alias	Age (years)	Allele	
	1	2			1	2
L-18362	28	460	L-3657	52	49	332
L-14575	29	460	L-3656	56	315	330
L-18384	19	430	L-3501	74	19	329
L-17672	20	430	L-3344	54	54	328
L-17665	29	430	D11	49	100	325
L-20363	54	400	L-3479	51	52	325
L-15166	19	350	L-3013	65	19	325
L-15764	87	350	A10	87	19	290
L-14630	19	342	C3	49	27	282
L-10410	25	315	A5	42	19	257
L-15891	54	312				
L-15754	19	290				
L-15629	19	270				
L-15739	59	270				
L-15713	19	270				

*These samples have a $(GAAGGA)_n$ motif and are considered non-pathogenic.

Table S3. Summary of *FGF14* core haplotype shared by three Australian individuals with $(GAA)_{>250}$.

chr	POS	REF	ALT	SYMBOL	AF	Rs name	AA2766	AA2770	AA2831
chr13	102095119	C	T	FGF14	0.008	rs79181669	0/1	0/1	0/1
chr13	**102150076**	**C**	**T**	**FGF14**	**0.0218**	**rs72665334**	**0/1**	**0/1**	**0/1**
chr13	**102161575**	**$(GAA)_{50}$**	**$(GAA)_{>250}$**	**FGF14**	**-**	**-**	**$(GAA)_{289}$**	**$(GAA)_{348}$**	**$(GAA)_{>400}$**
chr13	102261142	G	A	FGF14	0.0154	rs117891033	0/1	0/1	0/1
chr13	102264941	T	C	FGF14	0.0297	rs72647446	0/1	0/1	0/1
chr13	102269434	C	T	FGF14	0.0291	rs72647448	0/1	0/1	0/1
chr13	102396542	G	C	FGF14	0.0771	rs9557860	0/1	0/1	0/1
chr13	102405672	A	G	FGF14	0.0891	rs72649411	0/1	0/1	0/1
chr13	102407597	C	T		0.0944	rs72649412	0/1	0/1	0/1
chr13	102412712	T	G		0.0903	rs17690152	0/1	0/1	0/1
chr13	102419917	G	T		0.0879	rs58913166	0/1	0/1	0/1
chr13	102432196	G	A		0.0914	rs61593134	0/1	0/1	0/1
chr13	102435740	A	G		0.091	rs2182843	0/1	0/1	0/1
chr13	102439745	C	T		0.0228	rs4772471	0/1	0/1	0/1
chr13	102440446	T	C		0.0795	rs114317848	0/1	0/1	0/1
chr13	102440534	G	A		0.099	rs66678179	0/1	0/1	0/1
chr13	102441121	T	C		0.0795	rs72649438	0/1	0/1	0/1
chr13	102444527	G	A		0.0797	rs72649442	0/1	0/1	0/1
chr13	102446132	T	C		0.0801	rs57911285	0/1	0/1	0/1
chr13	102446353	A	T		0.0781	rs57461252	0|1	0|1	0|1
chr13	102446354	A	C		0.0795	rs60040500	0|1	0|1	0|1
chr13	102447030	C	T		0.0863	rs116926265	0/1	0/1	0/1
chr13	102447183	A	G		0.0801	rs117258042	0/1	0/1	0/1
chr13	102448603	G	C		0.0801	rs1927360	0|1	0/1	0/1
chr13	102448793	A	T		0.0801	rs1927361	0/1	0/1	0/1
chr13	102451762	C	T		0.0799	rs55665569	0/1	0/1	0/1
chr13	102453431	A	G		0.0813	rs12585989	0/1	0/1	0/1
chr13	102457322	T	G		0.0801	rs55686828	0/1	0/1	0/1
chr13	102465342	T	C		0.0825	rs55638789	0/1	0/1	0/1
chr13	102472363	G	A		0.0731	rs72649478	0|1	0|1	0|1
chr13	102473510	G	T		0.0996	rs72649480	0/1	0/1	0/1
chr13	102474084	A	G		0.091	rs114125113	0/1	0/1	0/1
chr13	102474982	A	T		0.0968	rs77919312	0|1	0|1	0|1
chr13	102476968	C	T		0.0729	rs56164689	0/1	0/1	0/1
chr13	102478700	C	T		0.0713	rs72649487	0/1	0/1	0/1
chr13	102478941	T	C		0.0783	rs72649488	0/1	0/1	0/1
chr13	102479117	C	T		0.0783	rs55850322	0/1	0/1	0/1
chr13	102480213	T	C		0.0713	rs56287885	0/1	0/1	0/1
chr13	102481686	A	AG		0.0723	rs55728938	0/1	0/1	0/1
chr13	102489485	C	T		0.0951	rs17634018	0/1	0/1	0/1
chr13	102491020	T	C		0.0649	rs17634060	0/1	0/1	0/1

Supplementary Materials and Methods

RNA and protein analyses

Primary fibroblasts were established from three affected individuals and four unrelated sex and age matched controls using standard techniques. Cells were cultured as previously described[1] with RNA extracted (RNeasy Mini Kit, #74104, QIAGEN) and cDNA generated (QuantiTect Reverse Transcription Kit, #205313, QIAGEN) according to the manufacturer's instructions. Gene expression was analyzed using TaqMan Gene Expression Assays designed to identify all *FGF14* mRNA isoforms (Hs00738588, Thermo Fisher Scientific) or specifically the brain isoform 1b (Hs02888324, Thermo Fisher Scientific) according to the manufacturer's protocol. Protein was isolated and analyzed by Western blot as previously described[2] utilizing an antibody directed against FGF14 (UC Davis/NIH NeuroMab, #75-096).

Supplementary References

1. Wilson, G.R., Sunley, J., Smith, K.R., Pope, K., Bromhead, C.J., Fitzpatrick, E., Di Rocco, M., van Steensel, M., Coman, D.J., Leventer, R.J., et al. (2013). Mutations in SH3PXD2B cause Borrone dermato-cardio-skeletal syndrome. European journal of human genetics : EJHG. 10.1038/ejhg.2013.229.
2. Barbier, M., Bahlo, M., Pennisi, A., Jacoupy, M., Tankard, R.M., Ewenczyk, C., Davies, K.C., Lino-Coulon, P., Colace, C., Rafehi, H., et al. (2022). Heterozygous PNPT1 Variants Cause Spinocerebellar Ataxia Type 25. Annals of neurology *92*, 122-137. 10.1002/ana.26366.